

DTIC FILE COPY

AD-A220 822



AFWAL-TR-89-4007

OXIDATIVE DEGRADATION OF ACETYLENE TERMINATED
SULFONE (ATS) RESIN

W. T. K. Stevenson
I. J. Goldfarb
E. J. Soloski

Polymer Branch
Nonmetallic Materials Division

DTIC
ELECTE
APR 24 1990
S D

10 January 1990

Final Report for Period January 1981 to June 1983

Approved for Public Release; Distribution Unlimited

MATERIALS LABORATORY
WRIGHT RESEARCH AND DEVELOPMENT CENTER
AIR FORCE SYSTEMS COMMAND
WRIGHT-PATTERSON AIR FORCE BASE, OHIO 45433-6533


90 04 23 022

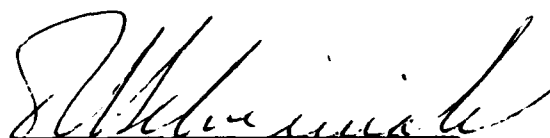
NOTICE

WHEN GOVERNMENT DRAWINGS, SPECIFICATIONS, OR OTHER DATA ARE USED FOR ANY PURPOSE OTHER THAN IN CONNECTION WITH A DEFINITELY GOVERNMENT-RELATED PROCUREMENT, THE UNITED STATES GOVERNMENT INCURS NO RESPONSIBILITY OR ANY OBLIGATION WHATSOEVER. THE FACT THAT THE GOVERNMENT MAY HAVE FORMULATED OR IN ANY WAY SUPPLIED THE SAID DRAWINGS, SPECIFICATIONS, OR OTHER DATA, IS NOT TO BE REGARDED BY IMPLICATION, OR OTHERWISE IN ANY MANNER CONSTRUED, AS LICENSING THE HOLDER, OR ANY OTHER PERSON OR CORPORATION; OR AS CONVEYING ANY RIGHTS OR PERMISSION TO MANUFACTURE, USE, OR SELL ANY PATENTED INVENTION THAT MAY IN ANY WAY BE RELATED THERETO.

THIS REPORT HAS BEEN REVIEWED BY THE OFFICE OF PUBLIC AFFAIRS (ASD/PA) AND IS RELEASABLE TO THE NATIONAL TECHNICAL INFORMATION SERVICE (NTIS). AT NTIS, IT WILL BE AVAILABLE TO THE GENERAL PUBLIC INCLUDING FOREIGN NATIONS.

THIS TECHNICAL REPORT HAS BEEN REVIEWED AND IS APPROVED FOR PUBLICATION.


R. C. EVERS
Polymer Branch
Nonmetallic Materials Division


T. E. HELMINIAK, Chief
Polymer Branch
Nonmetallic Materials Division

FOR THE COMMANDER


MERRILL L. MINGES, Director
Nonmetallic Materials Division

If your address has changed, if you wish to be removed from our mailing list, or if the addressee is no longer employed by your organization, please notify WRDC/MLBP, Wright-Patterson AFB, OH 45433-6533 to help us maintain a current mailing list.

Copies of this report should not be returned unless return is required by security considerations, contractual obligations, or notice on a specific document.

UNCLASSIFIED

SECURITY CLASSIFICATION OF THIS PAGE

REPORT DOCUMENTATION PAGE

Form Approved
OMB No. 0704-0188

1a. REPORT SECURITY CLASSIFICATION Unclassified			1b. RESTRICTIVE MARKINGS		
2a. SECURITY CLASSIFICATION AUTHORITY			3. DISTRIBUTION/AVAILABILITY OF REPORT Approved for public release; distribution unlimited		
2b. DECLASSIFICATION/DOWNGRADING SCHEDULE					
4. PERFORMING ORGANIZATION REPORT NUMBER(S) AFWAL-TR-89-4007			5. MONITORING ORGANIZATION REPORT NUMBER(S)		
6a. NAME OF PERFORMING ORGANIZATION Materials Lab, WRDC, AFSC		6b. OFFICE SYMBOL (If applicable) WRDC/MLBP		7a. NAME OF MONITORING ORGANIZATION	
6c. ADDRESS (City, State, and ZIP Code) Wright-Patterson AFB, OH 45433-6533				7b. ADDRESS (City, State, and ZIP Code)	
8a. NAME OF FUNDING/SPONSORING ORGANIZATION same as 6a		8b. OFFICE SYMBOL (If applicable)		9. PROCUREMENT INSTRUMENT IDENTIFICATION NUMBER	
8c. ADDRESS (City, State, and ZIP Code)				10. SOURCE OF FUNDING NUMBERS	
PROGRAM ELEMENT NO. 61102F		PROJECT NO. 2303		TASK NO. Q3	
				WORK UNIT ACCESSION NO. 07	
11. TITLE (Include Security Classification) Oxidative Degradation of Acetylene Terminated Sulfone (ATS) Resin					
12. PERSONAL AUTHOR(S) W.T.K. Stevenson, I.J. Goldfarb, and E.J. Soloski					
13a. TYPE OF REPORT Final		13b. TIME COVERED FROM Jan 81 TO Jun 83		14. DATE OF REPORT (Year, Month, Day) January 1990	
15. PAGE COUNT 95					
16. SUPPLEMENTARY NOTATION					
17. COSATI CODES			18. SUBJECT TERMS (Continue on reverse if necessary and identify by block number)		
FIELD	GROUP	SUB-GROUP			
07	04				
11	04		Polymers, resins, degradation, oxidation		
19. ABSTRACT (Continue on reverse if necessary and identify by block number) Acetylene terminated sulfone resin (ATS), prepared for the Air Force by Gulf Chemicals, Inc., hereafter designated as ATS-G, and components of that resin mixture isolated by column chromatography, were exposed to elevated temperatures in the presence of oxygen to determine and compare oxidative stabilities. Degradation in the presence of an unlimited supply of oxygen was simulated by programmed thermogravimetry, and under partially anaerobic conditions, by using a reactor of novel design built for that express purpose. For example, it was found by thermogravimetry (TGA) that although oxygen does not appear to be incorporated to any measurable extent into ATS polymers cured in air, those polymers became slightly less resistant to high temperature oxidative degradation than their counterparts cured under nitrogen. In other experiments, it was shown that direct attack of oxygen on ATS resins, at least under the conditions of the TGA experiment, takes place only after completion of those thermal degradation reactions producing oligomeric and condensable volatile products of degradation. In other words, the stability of those resins to oxidation under the accelerative conditions					
20. DISTRIBUTION/AVAILABILITY OF ABSTRACT <input checked="" type="checkbox"/> UNCLASSIFIED/UNLIMITED <input type="checkbox"/> SAME AS RPT. <input type="checkbox"/> DTIC USERS			21. ABSTRACT SECURITY CLASSIFICATION Unclassified		
22a. NAME OF RESPONSIBLE INDIVIDUAL R. C. Evers			22b. TELEPHONE (Include Area Code) 513-255-9161		22c. OFFICE SYMBOL WRDC/MLBP

19. of the TGA experiment is proportional to their thermal stability. In a parallel set of experiments conducted with the polymer in contact with a fixed small amount of oxygen to crudely simulate those conditions encountered within a fiber-reinforced composite, we showed that under accelerative conditions and at high temperatures, the resin (or its residue of thermal degradation) possesses a higher oxidative stability than early products of its own thermal degradation, which "scavenge" oxygen to form secondary products such as carbon monoxide, carbon dioxide, and water, thus preventing direct oxidation of the composite matrix.

- (11)

ACKNOWLEDGEMENTS

The authors would like to thank Mr J. Henes for his technical help and Mr R. Grant who fabricated most of the free-standing glassware described here. In addition, W. T. K. Stevenson would like to thank the National Research Council for its support in the provision of a Research Associateship for him at WPAFB.



Accession For	
INTS CRA&I	<input checked="" type="checkbox"/>
DTIC TAB	<input type="checkbox"/>
Unannounced	<input type="checkbox"/>
Justification	
By	
Distribution /	
Availability Codes	
Dist	Availability Codes
A-1	

TABLE OF CONTENTS

SECTION	PAGE
I Introduction	1
II Chemical Characterization of ATS Polymers	4
III Thermal Degradation of ATS-G	5
1. Thermal Volatilization Analysis (TVA) and Gravimetric Analysis	6
2. Sub Ambient Thermal Volatilization Analysis (SATVA)	8
3. Quantitative Product Distribution	9
IV Thermogravimetric Analysis (TGA) in Air of ATS Polymers	11
1. TGA of ATS-G and its Components in Air and Under Helium	12
2. TGA in Air of Precured and Uncured ATS-G and its Component Fractions	15
3. TGA in Air of Thermally Degraded ATS-G	16
V Development and Use of the Oxidation Reactor	18
1. Description of the Reactor	19
2. Description of the Experiment	20
3. Oven Calibration	21
4. Sample Preparation	22
5. Gas Flow in the Reactor	22
6. Reactor Volume Calibration and Oxygen Measurement	23
7. Oxygen Purification	24
8. System Leakage and Gas Purity Check	25
9. Condensable Gas Trapping Efficiency	26
10. Product Analysis	29
a. The Residue of Oxidation	29
b. The Oligomeric Product Fraction of Oxidation	29
c. The Condensable Volatile Product Fraction of Oxidation	29
d. The Noncondensable Volatile Product Fraction of Oxidation	30
VI Oxidation of ATS-G Under Closed System Conditions	31
1. SATVA of the Condensable Volatile Products of Oxidation to 800°C	32
2. Gravimetric Analysis of the Residues of Oxidation to 800°C	33
3. Oligomer Product Analysis	34

SECTION		PAGE
VI	4. Quantitative Volatile Product Distributions of Oxidation to 800°C	35
	5. Oxidation of Thermally Degraded ATS-G	38
	6. Translation to a Composite Environment	40
	Conclusions	42
	References	46
	Figures	47-84

LIST OF FIGURES

FIGURE		PAGE
1	TVA to 1020°C of Uncured ATS-G	48
2	% Residue of Vacuum Degradation of Uncured ATS-G	49
3	SATVA of Condensable Volatile Products of Thermal Degradation to 1020°C of Precured ATS-G	50
4	TGA of ATS-G in Air and Under Helium	51
5	TGA of ATS Monomer in Air and Under Helium	52
6	TGA of ATS Dimer in Air and Under Helium	53
7	TGA of ATS Trimer in Air and Under Helium	54
8	TGA of F4 in Air and Under Helium	55
9	TGA of F5 in Air and Under Helium	56
10	TGA of F7 in Air and Under Helium	57
11	A Comparison Between Solvent Compensated TGA Curves in Air for Uncured ATS-G and its Components	58
12	TGA in Air of Precured and Uncured ATS-G	59
13	TGA in Air of Precured and Uncured ATS Monomer	60
14	TGA in Air of Precured and Uncured ATS Dimer	61
15	TGA in Air of Precured and Uncured ATS Trimer	62
16	A Comparison Between TGA Curves in Air for Precured ATS-G and its Component Fractions	63
17	TGA in Air of ATS-G, Predegraded Under Helium to 600°C	64
18	TGA in Air of ATS-G, Predegraded Under Helium to 700°C	65
19	TGA of Graphite in Air	66
20a	Oxidation Reactor	67
20b	Key to Figure 20a	68
21	Vacuum Manifold Schematic	69
22	Assembly for Oven Calibration	70
23	Oven Calibration Curve for Oxidation Reactor	71
24	Gas Purification Train Schematic	72
25	Gas Manipulation Manifold	73
26	SATVA of Condensable Volatiles Collected in Blank Run to 800°C	74
27	Calibrated Container for Quantitative Gas Phase I. R. Analysis of Condensable Volatile Products of Oxidation	75
28	Gas Phase I. R. Spectra of Carbon Dioxide, Before and After Expansion into Calibrated Container	76
29	Gas Phase I. R. Spectrum of the Condensable Volatile Products of Oxidation to 800°C of Precured ATS-G	77
30	Proton N. M. R. Spectrum of the Condensable Volatile Products of Oxidation to 800°C of Precured ATS-G	78
31	Gas Phase I. R. Spectrum of the Noncondensable Volatile Products of Oxidation to 800°C of Precured ATS-G	79
32	SATVA of Condensable Volatile Products of Oxidation to 800°C of 50mg Precured ATS-G	80
33	SATVA of Condensable Volatile Products of Oxidation to 800°C of 100mg Precured ATS-G	81
34	I. R. Spectrum of the Oligomeric Product Fraction of Oxidation to 800°C of Precured ATS-G	82

LIST OF FIGURES (Cont'd)

35	I. R. Spectrum of the Oligomeric Product Fraction of Thermal Degradation to 1020°C of Precured ATS-G	83
36	SATVA of Condensable Volatile Products of Oxidation to 700°C of ATS-G, Predegraded Under Vacuum to 700°C	84

LIST OF TABLES

TABLES		PAGE
1	Quantitative Analysis of the Products of Thermal Degradation to 1020°C of ATS-G	11
2	Temperatures Corresponding to the Onset and Rate Maxima of Processes Observed in the TGA Curves of Uncured ATS Polymers	13
3	Temperatures Corresponding to the Onset and Rate Maxima of Oxidative Processes in Predegraded ATS-G	17
4	Efficiency of Recovery of Carbon Dioxide from 5A Molecular Sieve at Room Temperature	28
5	Residues of Thermal and Oxidative Degradation of ATS-G to 800°C at 5°C/min	33
6	Product Distribution of Closed System Oxidation to 800°C of 50mg ATS-G	36
7	Product Distribution of Closed System Oxidation to 800°C of 100mg ATS-G	36
8	Wt.% Carbon Volatilized from ATS-G Degraded Under Vacuum and in Oxygen	37
9	Carbon Dioxide/Carbon Monoxide Product Ratios of Oxidation to 800°C of ATS-G	38
10	A Product Distribution for the High Temperature Bulk Oxidation Reaction of ATS-G	39

SECTION I

INTRODUCTION

As part of a long term effort to upgrade the technologies associated with the manufacture of advanced fiber reinforced composite materials, the Air Force has expended much effort devoted to the development of viable alternatives to the epoxy resins, which are still the matrices of choice for most such applications. To this end, resins formed through the polymerization of acetylenes have received much attention due to their higher thermal stability, and ability to cure or thermally crosslink in the absence of added hardener.

Most of the Acetylene Terminated or AT resin formers investigated by the Polymer Branch, WRDC, have consisted of short chain linear oligomers in the molecular weight range (200-1000) Daltons, capped at either end with a terminal acetylene group. Most synthetic work has concentrated upon variations of molecular weight distributions and of structure between the end caps. Characterization of candidate resins has generally followed the twin thrusts of thermal stability and mechanical measurements on the base resin and simple composite test pieces from that resin, if warranted.

One such resin, generally termed Acetylene Terminated Sulfone or ATS, due to the central bridging sulfones of the bisphenol moiety used to form the "backbone" of the resin, was deemed of

sufficient interest to arrange for its synthesis on a pilot plant scale. This contract, successfully completed by Gulf Chemicals Inc.⁽¹⁾, resulted in an ample supply of the resin, here designated as ATS-G, for subsequent evaluation. As expected, the resin was subjected to a battery of sophisticated mechanical and rheological tests to form a data base for an evaluation of structure/property parameters⁽²⁾. In concert, a detailed chemical analysis of prepolymer structure was made, followed by determination of structure-stability correlations, achieved by the application of a range of thermo-analytical techniques to the problem of deducing the rates and mechanisms of thermal degradation of the cured resin in a high vacuum or under a helium blanket. The end result of this analysis was expected to be an identification of thermal "weak links" in the resin to guide us in future syntheses of more stable precursors. A chemical, and preliminary thermal characterization of the ATS-G resin was reported in an earlier Air Force Technical Report⁽³⁾. Subsequently, we reported a more detailed thermal analysis of the system⁽⁴⁾.

Although intrinsically useful, the results of polymer thermal degradation studies are only indirectly applicable to predictions of resin lifetimes and stabilities, because, of course, such materials, in use, are exposed to oxygen at elevated temperatures. For this reason, to complete the thermal characterization of the ATS system, we performed some thermal analyses in air, the results of which are reported here.

Essentially, ATS-G and isolated components of that resin mixture with differing thermal histories were subjected to programmed degradation under air, and weight losses were measured and compared by thermogravimetry. By so doing, we were able to establish some structure-stability trends for the accelerated oxidations of this class of material.

On a more fundamental level, we became intrigued by the ongoing controversy with regards to the applicability of accelerated thermal testing under vacuum or inert atmosphere to the corresponding problem of materials stability in air. Only in some instances has any consensus of opinion emerged in the thermal analysis community on the applicability of accelerated inert atmosphere testing to the problem of oxidative stability. This issue is, of course, of interest in our laboratories due to the reliance upon such tests for the rapid evaluation and "grading" of the stabilities of new polymers and composites as they are synthesized. For example, it is rightly held that such comparisons are invalid at temperatures where reactions are slow, and where the presence of oxygen completely changes the course of degradation. Good examples of this phenomenon would be long term polyolefin and polydiene oxidation. Most contentious is still the issue of the use of accelerated thermal testing under inert atmospheres for the grading of resistances to rapid oxidation or burning. Some contend that volatile products of thermal degradation of polymers, through rapid gas phase oxidations (burning) denude the polymer surface of oxygen, to encourage thermal degradations as the primary decompo-

sition process, especially of thick parts where oxygen diffusion problems are encountered; while others contend that oxygen, even at very low concentrations, is still able to play a significant part in the primary decomposition process.

To resolve to our satisfaction, the thermal or oxidative nature of the primary decomposition reactions of the class of highly crosslinked thermally stable resins of interest to the Air Force, we devised a degradation reactor for the accelerated decomposition of such resins in the presence of small and carefully metered amounts of oxygen. We initially chose to probe, with some interesting results, the effects of small amounts of oxygen on the decomposition reactions of ATS resin, due to the large data base already accumulated on its thermal decompositions^(3,4).

SECTION II

CHEMICAL CHARACTERIZATION OF ATS POLYMERS

ATS resin, as prepared by Gulf Chemicals Inc., was separated into its component fractions by preparative scale column chromatography, the details of which are reproduced in an earlier Air Force Technical Report⁽³⁾. Essentially, the resin was shown to consist of a mixture of species comprising the monomer, some solvent and anomalous low molecular weight contaminants, the dimer and trimer in decreasing proportions, and some anomalous monomeric

and higher molecular weight by-products of synthesis. At first, we were concerned with the effect of these anomalous species on the thermal stability of the resin mixture. In truth, their effect on the resin proved to be minimal, the mixture possessing a thermal stability somewhere between the pure monomer and dimer⁽⁴⁾. In this report we comment on, among other things, the effect of backbone chain length and impurity content on the oxidative stability of that same resin system and its individual component fractions.

SECTION III

THERMAL DEGRADATION OF ATS-G

A number of conclusions drawn from this work are based upon comparisons between the thermal and oxidative degradation of ATS polymers. For this reason, we feel it necessary to expound upon salient features of the thermal decomposition of ATS resins, before progressing to a discussion of their oxidative degradation. In the main, information reproduced here has been drawn from previous Air Force Technical Reports^(3,4).

1. Thermal Volatilization Analysis (TVA) and Gravimetric Analysis

The Thermal Volatilization Analysis or TVA experiment centers upon the programmed warm-up of a polymer sample under high vacuum

conditions. The degradation tube is connected to the pumping system through a glass fractionation manifold consisting of a series of "U" traps chilled to progressively lower subambient temperatures, each bracketed by electronic Pirani pressure gauges. By use of this experiment, it therefore becomes possible to not only record the rate profile of volatile formation in the polymer as a function of temperature, but also to gain some insight into the composition, or more precisely, the volatility, of the products of degradation. A TVA trace for uncured ATS-G is reproduced in Figure 1. A corresponding weight loss curve for the same polymer is shown in Figure 2. In this experiment the uncured resin was warmed into the quartz sample container then cured in place by programmed heating during the early stages of the TVA experiment. We have divided both the TVA and the weight loss curve into four temperature regions based on earlier results⁽⁴⁾.

a. Room Temperature - 250°C

In this temperature interval the resin chemically crosslinks to a dense infusible mass. Volatiles produced in this interval correspond to solvent and some higher molecular weight species which are evaporated from the sample prior to its vitrification.

b. 250°C - 400°C

In this temperature interval the resin undergoes, as yet poorly understood, post cure processes. A very small, perhaps insignificant, fraction of the resin is volatilized in this temperature interval.

c. 400°C - 600°C

A mixture of condensable volatile and higher molecular weight degradation products (approximately 40% by weight of the sample) are evolved from the polymer in this temperature interval. In truth, two consecutive processes have been identified as operative in this temperature interval.

The first such process is instigated by initial sulfone bond scissions in the polymer to produce sulfur dioxide as a gaseous product, along with some phenol, formed by the scission of adjacent phenolic ethers to produce radicals which are stabilized by resonance into the sulfone group. In addition, some higher oligomers are produced by evaporation from the polymer of long segments from ATS dimer and higher species, arising from multiple sulfone bond scissions in higher ATS oligomers which "chop the chain" to volatilize these high molecular weight segments. The second process involves the less discriminate removal of phenyl and polyphenylethers from the polyene backbone of the resin (or its thermal derivative at that point) as benzene and water. In this text, we will show that the products of these two separate but overlapping processes can delay the onset of accelerated oxidations

of the polymer by reacting with and removing oxygen from the polymer surface.

d. 600°C - 1000°C

In this temperature interval relatively small amounts of hydrogen, carbon monoxide, and methane are removed from the polymer, in concert with the polyaromatizations and ring fusions which dominate at this stage of the degradation process. The inordinately high pressure readings recorded here reflect the very high Pirani responses of these small molecules.

2. Sub Ambient thermal Volatilization Analysis (SATVA)

Sub Ambient Thermal Volatilization Analysis or SATVA consists of a simple "add on" to the TVA experiment in which condensable volatiles produced in the latter are routed to a "U" tube on the vacuum line which is encased in paraffin wax and held at -196°C by immersion in liquid nitrogen. Once condensed in the tube, the liquid nitrogen is removed and the "U" tube allowed to slowly warm to room temperature. In so doing, the condensable volatile products of degradation, which had been condensed in the "U" tube, are separated by evaporation from that tube in order of volatility, without having to first remove material from the vacuum line. The tube temperature and the Pirani output from a neighboring pressure gauge are recorded over the period of the experiment to yield the SATVA trace corresponding to the condensable volatile products of

polymer degradation. Material evolved from the tube is then routed to other limbs of the TVA fractionating grid for spectroscopic and other analysis. An SATVA trace corresponding to the condensable volatile product fraction of degradation of ATS-G in the temperature interval RT-1020°C is reproduced in Figure 3. The large amounts of sulfur dioxide and phenol produced by early bond scissions in the polymer are clearly evident, as are the smaller, but still significant amounts of benzene and water which are produced in the later processes. Carbon dioxide and carbonyl sulfide are products of more esoteric reactions which need not concern us here.

3. Quantitative Product Distribution

The products of thermal degradation to 1020°C of ATS-G were analyzed by quantitative gas phase Infrared (IR) spectroscopy, by quantitative proton Nuclear Magnetic Resonance (NMR) spectroscopy, and by gravimetry, as previously outlined⁽⁴⁾. A knowledge of this product distribution is essential to a successful interpretation of the results of the closed system oxidations reported here. As such, the product distribution of thermal degradation to 1020°C of ATS-G is reproduced in Table 1, along with an itemized listing of the associated losses of carbon from the polymer which accompany the volatilization process, for subsequent reference to Section VI of this report.

TABLE 1 QUANTITATIVE ANALYSIS OF THE PRODUCTS OF THERMAL DEGRADATION TO 1020°C OF ATS-G

PRODUCT	Wt% of CURE POLYMER	VOLATILIZED CARBON (100mg) CURED POLYMER
H ₂	Negligible	0.0
CH ₄	3.0	2.2
CO ₂	6.2	2.7
CO	1.2	0.3
CO ₂	1.2	0.2
SO ₂	10.7	0.0
Benzene	2.2	2.0
H ₂ O	5.0	0.0
Phenol	11.9	9.1
Oligomeric Material	6.5	5.1
TOTAL	47.9	21.6

SECTION IV

THERMOGRAVIMETRIC ANALYSIS (TGA) IN AIR OF ATS POLYMERS

We first used programmed Thermogravimetry (TGA) as an accelerated test to determine and compare the stabilities of previously uncured ATS-G and its component fractions in air and under nitrogen. We next compared, by this method, the oxidative stabilities of ATS resin which was air cured in-situ in the TGA experiment, to that of ATS which had been precured under nitrogen. We finally isolated the high temperature bulk oxidation reaction of ATS polymers by oxidizing resin which had been predegraded under nitrogen. The rationale behind these experiments, and results so obtained, are reproduced below.

For ease of comparison, each TGA weight loss curve is divided into the four temperature intervals specified in Section III of this report.

RT-250°C:	CURE
250°C-400°C:	POST CURE
400°C-600°C:	STEP 1 OF DEGRADATION
ABOVE 600°C:	STEP 2 OF DEGRADATION

1. TGA of ATS-G and its Components in Air and Under Helium

We, first of all, compared the TGA curves from uncured ATS-G and its component fractions which had been heated in air and under a helium atmosphere. These weight loss curves are reproduced in Figures 4-10.

The polymerization of acetylenes to a polyene crosslink is a free radical based process⁽⁵⁾. As such, we expected that the polymerization reaction would be influenced somewhat by the presence of oxygen⁽⁶⁾. From the similarities in the initial portions of the weight loss curves of resins degraded in air and under nitrogen, it becomes apparent that oxygen is not copolymerized with the polyene to any great extent. (However, even trace quantities of oxygen can alter the course of free radical processes, and it was not surprising to find that acetylene terminated resin prepared in the presence of oxygen possessed somewhat differing physical properties than the same resin prepared under an inert atmosphere⁽²⁾).

From the TGA curves, it can be seen that oxygen does participate in the process designated as Step 1 of degradation of ATS polymers. As resin appears from these experiments to be more stable to early degradations under an oxygen atmosphere than under nitrogen, it may be that the former is able to add to radicals produced by homolytic scissions in the resin, to retard the buildup of a destructive radical population in the material. At higher temperatures, oxygen appears to directly attack the polymeric residue to completely volatilize that residue. It is interesting to note that the apparent onset of this bulk oxidation reaction seems to coincide with the end of that temperature interval corresponding to Step 1 of thermal degradation of all seven resins examined here. This may indicate that the high temperature bulk oxidation of ATS-G and its component fractions is inhibited by the volatile products of Step 1 of thermal or oxidative degradation, either chemically through a suppression of radical activity, or physically by a depletion of oxygen at the polymer surface by secondary gas phase oxidations of those products. The proximity between the "end" and "onset" temperatures so discussed is illustrated in Table 2.

TABLE 2 TEMPERATURES CORRESPONDING TO THE ONSET AND RATE MAXIMA OF PROCESSES OBSERVED IN THE TGA CURVES OF UNCURED ATS POLYMERS

MATERIAL	END OF STEP 1 OF THERMAL DEGRADATION	START OF BULK OXIDATION REACTION	RATE MAXIMUM OF BULK OXIDATION REACTION
ATS-G	600	585	635
ATS MONOMER	580	585	635
ATS DIMER	585	580	630
ATS TRIMER	585	600	620

F4*	545	570	630
F5*	540	535	600
F7*	370	390	480

*Anomalous species isolated from the ATS-G resin mixture by column chromatography, and more fully described in reference #3.

As an alternative explanation to this phenomenon, we may postulate that the initial resin is more oxidatively stable than residual products of thermal degradation, and it is only upon formation of the latter that the bulk oxidation reaction can take place. However, the thermal stabilities of organics are known to generally decrease with increasing heteroatom content, and to reach a maximum in pure carbon, of which the residue of Step 1 of thermal degradation is a reasonably good approximation. Evidence to support the first explanation, that the bulk oxidation reaction is suppressed by gas phase oxidation of products of thermal degradation of the resin, is presented in Section IV of this report.

The effect of crosslink density in the initial polymer on oxidative stability can be estimated by simple superposition for comparative purposes of solvent compensated TGA weight loss curves obtained in air, and such is performed in Figure 11, from which it can be seen that aside from the anomalous fraction designated as F5, all weight loss curves are similar in profile. This supports earlier long term aging studies of these resins in air, which suggest even greater similarities in oxidative stability at lower temperatures and over longer time periods⁽³⁾.

2. TGA in Air of Precured and Uncured ATS-G and its Component Fractions

We previously mentioned that oxygen may participate in the acetylene polymerization reaction, although such incorporation was not detectable by gravimetry. To test for the effect (if any) of incorporation of oxygen into the polyene chain on the high temperature oxidative stability of ATS resins; ATS-G, monomer, dimer, and trimer, were cured under high vacuum conditions at a heating rate of 5°C/min to simulate the thermal history of resin cured in the TGA pan, but without the oxygen. The weight loss curves of those resins were then compared with those cured in-situ and degraded under air in the TGA pan. Such comparisons are reproduced in Figures 12-15, from which it can be seen that the material precured under nitrogen is more stable to high temperature oxidations than corresponding material cured then degraded in air. TGA curves in air of precured ATS-G, monomer, dimer, and trimer are compared in Figure 16, from which it can be seen that these materials possess a same relative ordering of stability to oxidation as the uncured resin.

Although some resin fractions do lose a low molecular weight component when heated under vacuum (ATS monomer being a prime example) with a corresponding change of composition, and therefore possibly of stability, most do not; a prime example being ATS dimer which does not lose any weight when heated under vacuum, but which appears to form an appreciably more stable resin when cured in the absence of air.

We may speculate on the most probable reasons for differences in stability between the two systems. To begin with, we have previously shown that ATS resins are appreciably more thermally stable than their thermoplastic counterparts such as Radeltm polysulfone resin⁽⁴⁾, an extra stability we attributed to the presence of polyene crosslinks in the resin which appear to act as nuclei for the high temperature polyaromatizations which transform such resins into carbon char. If, as surmised, oxygen is somehow incorporated into a polymerizing polyene to perhaps form a peroxidic linkage, then such a linkage would subsequently break at higher temperatures, to disrupt those polyenes and lessen their ability to "catalyze" oxidatively stable char formation.

3. TGA in Air of Thermally Degraded ATS-G

As mentioned earlier, the close proximity between the cessation of the first process of thermal degradation of these polymers and the onset of the bulk oxidation reaction is worth mention, because it suggests that the oxidation reaction is suppressed by gas phase oxidation of a "blanket" of volatiles produced by the first processes of thermal degradation. This premise was reinforced through a separation of the two processes (thermal degradation and oxidative degradation) by predegrading polymer under helium to drive off the products of thermal degradation, cooling the char to room temperature, then reheating that residue in air. If the temperature profile of the bulk oxidation reaction is an intrinsic property of the material, then the high

temperature weight loss profiles should coincide. If, on the other hand, the weight loss profiles are significantly different, then credence would be lent to the hypothesis that the temperature profile of the bulk oxidation reaction is an artifact of this "blanketing" effect. Such experiments are reproduced in Figures 17 and 18, which depict the effect on the position and profile of the bulk oxidation reaction of predegradation under argon to 600°C and 700°C respectively. Important features of both curves are summarized in Table 3.

TABLE 3 TEMPERATURES CORRESPONDING TO THE ONSET AND RATE MAXIMA OF OXIDATIVE PROCESSES IN PREDEGRADED ATS-G

EXPERIMENTAL CONDITIONS	ONSET OF OXIDATION REACTION (°C)	ONSET OF RAPID OXIDATION (°C)	RATE MAXIMUM OF BULK OXIDATION REACTION (°C)
Predegraded to 600°C	465	535	555
Predegraded to 700°C	455	525	550

The two oxidative weight loss curves shown in Figures 17 and 18 are similar in profile, to show that thermal rearrangements in ATS-G char between 600°C and 700°C (if any) do not markedly change its absolute stability to oxidation. By comparing these curves with the composite thermal/oxidative curve for the same polymer depicted in Figure 4, it can be seen that the bulk oxidation reaction of ATS-G is indeed upshifted or suppressed by Step 1 of thermal degradation, as suggested earlier in this report.

At 600°C or 700°C, ATS-G has been transformed by thermal

processes into a residue of almost pure carbon which contains only trace amounts of hydrogen, oxygen, and sulfur. Its microstructure, which is reflected in oxidative stability, is however, much different from graphite, a TGA curve of which is depicted in Figure 19. Step 1 of thermal degradation of ATS-G quantitatively fractures the resin on a molecular scale to produce a disordered char with a high surface area. As such, a high internal surface area is available for reaction with oxygen, to lower the effective oxidative stability of the char below that of graphite.

SECTION V

DEVELOPMENT AND USE OF THE OXIDATION REACTOR

Encouraged by the results of our TGA experiments, which appeared to suggest that the primary decomposition reaction in these highly stable polymers was thermal in nature, we set out to construct a reactor with which to study more closely the high temperature decomposition reactions of ATS and other such resins.

We chose to develop a system operable at reduced pressures for ease of coupling to a glass vacuum manifold, that products of degradation be amenable to subsequent chemical analysis. An added advantage of so doing, is that conditions of restricted oxygen access to the resin, as would be found within a part of some thickness, can be simulated. To our knowledge, such equipment could not be purchased, and so we set out first of all, to develop the opera-

ting requirements for such a reactor, to design and build a reactor meeting those requirements, and finally, to test its operation. Details of this progression form the basis of this section.

1. Description of the Reactor

The oxidation reactor, alluded to above, had to be operable at reduced pressures for reasons already mentioned in this text. For design purposes we decided that a closed system oxidation was also preferable in that the polymer could be made to react with precisely metered amounts of oxygen. However, allowance then had to be made to prevent a static buildup of unreactive gas at the polymer surface. In other words, a recirculating loop of gas had to be formed to maintain the efficiency of the oxidation process. In tandem, a method had to be developed to condense from the gas stream the volatile products of oxidation for their eventual analysis. Our final reactor design is illustrated in Figure 20, and its spatial relationship with other components of the degradation assembly is shown in Figure 21. Essentially, the reactor is connected to the vacuum pumps through the TVA fractionation grid already mentioned in Section III of this report. An oxygen cylinder is connected also to the reactor through a gas manipulation assembly, then to the TVA manifold. The operation of these component entities is discussed at some length elsewhere in this section.

2. Description of the Experiment

With reference to Figure 20, we may subsequently "define" the oxidation experiment as performed here. The sample to be oxidized is placed in a quartz crucible with fluted base, so designed to encourage air flow past the sample. The sample "boat" is then lowered into the open ended quartz degradation tube which is enclosed in the muffle furnace, then sealed at top and bottom "O" ring joints, into the static glassware assembly. The whole assembly is pumped to a hard vacuum, and prepurified oxygen (220mg) is then admitted to the reactor through the vacuum line. The cold traps are filled with liquid nitrogen, the heating tape and magnetic drive pump are switched on, and the assembly is heated to 700°C or 800°C at a programmed heating rate of 5°C/min. The oven is then switched off and lowered below the sample which is allowed to cool to 100-200°C. The condensable, noncondensable, oligomeric, and residual products of oxidation are then analyzed by methods described elsewhere in this section.

Having described the experiment per se, we will next discuss individually, such important experimental details as sample preparation, oven calibration, oxygen purification, and efficiencies of product recovery.

3. Oven Calibration

The heat source used throughout this work was a Marshall 2000°F tubular muffle furnace coupled to a West temperature programmer. All degradations were performed at a nominal heating rate of 5°C/min. Oven temperatures were recorded as a function of time using a Chromal Alumel thermocouple adjacent to the programmer controller.

The temperature of the polymer sample was always lower than that of the furnace because of the thermal lag between the furnace, the degradation tube, and the crucible. The relationship between the oven and sample temperature was obtained using the assembly shown in Figure 22 to produce the calibration curve drawn in Figure 23.

Simply put, a chromel alumel thermocouple was connected to the reactor through a ground glass joint, and threaded down to press firmly against the crucible surface. The entrance point was made temporarily vacuum tight with epoxy glue and sealing wax, and the reactor warmed at a heating rate of 5°C/min to an end point of 1020°C. Both the oven and the calibration thermocouple were connected to the same recorder, and temperature profiles recorded as corresponding millivolt outputs. Thereafter, sample temperatures at any point in the warmup curve could be deduced from the oven thermocouple trace by simple reference to that calibration curve.

4. Sample Preparation

Samples of ATS-G were deposited as thin films onto the base of quartz crucibles and cured by programmed heating at 5°C/min to 334°C under high vacuum conditions in the TVA apparatus, to produce solvent free polymer films which were stored at room temperature until used. The 50mg and 100mg samples used in this work produced films of average thickness 50 and 120 micrometers respectively, both of which are below the limit of 180 microns at which gas diffusion appears to begin to play a major role in the bulk oxidation process^(7,8).

5. Gas Flow in the Reactor

Gas, in contact with the degradation tube, expands, becomes less dense, and rises due to classic convection effects. In contrast, gas in contact with the cold traps contracts, becomes more dense, and falls. It was hoped that a circuit would be completed by gas flow through the horizontal connecting tubes, to produce a recirculating loop of gas powered by heat exchange from the oven to the cold traps. Unfortunately, the oven and cold traps produced isolated convection currents in the two vertical members of the reactor. We then wrapped the top cross member in electrical heating tape and installed a small water cooled magnetic drive pump into the assembly below the oven. The heating tape was maintained at 60-80°C and the pump was operated at 40 volts to produce a

gentle flow of gas through the system, which was confirmed by introduction of bromine to the reactor under reduced pressure at the feed through point mentioned in Part 3 of this section, and observing the slow one-way movement of the gas to the cold traps.

6. Reactor Volume Calibration and Oxygen Measurement

A volume calibrated storage bulb was attached to the assembly at the electrical feed through point of Figure 22, and the volume of the reactor assembly was determined to be (1229 ± 5) ml by simple gas expansion through application of Boyles law. To simplify matters, all degradation experiments were performed under an oxygen pressure of 1 cm of mercury. It can be shown that 220 mg of oxygen in the reactor produces a pressure corresponding to 1 cm Hg at room temperature. A 4% pressure drop was recorded when the heating tape was switched on and the cold traps were filled with liquid nitrogen. In all experiments, oxygen was introduced with the system at room temperature, in other words, with polymer initially in contact with 220 mg oxygen.

The pressure in the reactor increases with oven temperature as the degradation experiment progresses. Oxygen is, however, partially converted to condensable materials which are removed from the gas phase by condensation into the cold traps. The two effects tend to cancel with the result that the maximum pressure recorded in any experiment was 2 cm Hg. This is, of course, below the 15 cm pressure of oxygen gas required for condensation at -196°C , and so

problems of safety were never encountered. Even so, the mercury manometer, depicted in Figure 20, was left open to the atmosphere during the course of experiments as a potential pressure release valve.

7. Oxygen Purification

Oxygen was purified in the assembly shown in Figure 24, reference to which will be made throughout this discussion. The gas manipulation manifold as drawn in Figure 25, was connected to a cylinder of research grade oxygen through a vacuum stopcock, which was opened to admit the gas to that manifold. Gas was flushed through the manifold to exit through the manometer column for about 10 minutes. The gas storage reservoir was cooled to -196°C and approximately 5ml of liquid oxygen was condensed into the bulb. The system was isolated and a "top cut" of 1-2ml was flushed to the pumping system to remove contaminants from the system. A middle cut was then expanded from the reservoir at -196°C through an activated 5A molecular sieve trap held at room temperature, and a cold trap at -196°C (to remove traces of water and carbon dioxide from the gas flux) to the oxidation reactor, and shown schematically in Figure 24. The molecular sieve trap was then reactivated at 200°C under a high vacuum and made ready to receive the non-condensable volatile product fraction of oxidation as mentioned later in this section.

We may rationalize the purification steps as follows: Oxygen from the cylinder is contaminated with small amounts of nitrogen, carbon dioxide, and water. Nitrogen is an undesirable impurity because it is (in general) unreactive and can hamper diffusion of oxygen to the polymer surface. Carbon dioxide and water are also end products of the oxidation process and their presence in the feed mixture will lead to their improper measurement in the product distribution of the oxidation reaction. At a pressure of one atmosphere, nitrogen will not liquify at -196°C except in trace quantities which are purged to the pumping system with the "top cut" from the liquid oxygen. On the other hand, carbon dioxide and water are completely involatile at -196°C and once condensed into the liquid oxygen, remain there as long as the tube is held at -196°C . In other words, they do not evaporate with the middle cut into the oxidation reactor. Trace concentrations of these gases in the middle cut are further lowered by passage through a 5A molecular sieve trap held at room temperature and a cold trap held at -196°C .

8. System Leakage and Gas Purity Check

To perform properly, the reactor must be supplied with pure oxygen (by methods outlined in the previous section) and remain leak tight throughout the course of the experiment. We therefore had to determine the purity of gas introduced to the reactor and the leak rate of that reactor throughout the course of the experiment, as such impurity and leakage can introduce extraneous water

and carbon dioxide to the products of degradation. To do so, the following experiment was performed.

The reactor was assembled, pumped to a high vacuum (10^{-4} torr), sealed, and left for 24 hours. The reactor was then opened to a section of evacuated TVA manifold equipped with a Pirani gauge to measure pressure built up in the reactor over that time period. By this experiment it was estimated that leakage into the system occurred at a rate of less than 1mm Hg/24 hour period.

The reactor was assembled, pumped to a high vacuum (10^{-4} torr), and 220mg of purified oxygen was admitted. A blank run to 800°C was performed and condensable volatile "products" were examined by gravimetry in a preweighed gas tight container, by SATVA as illustrated in Figure 26, and by quantitative gas phase infrared spectroscopy. By these means it was shown that about 0.8mg of carbon dioxide and 0.5mg of "other material" accumulated in the reactor during the course of a blank run. Background levels of these "other" materials (presumably benzene and phenol, left in the reactor from prior experiments) were subsequently reduced by pre-evacuation for 48 hours prior to each experiment.

9. Condensable Gas Trapping Efficiency

To properly use the reactor described here it was essential that the condensable gas trapping efficiency in the cold traps be determined. Essentially, all the noncondensable volatile products of degradation are removed from the reactor at the end of the

experiment, through a liquid nitrogen cold trap, to the molecular sieve containing trap also held at -196°C . A poor trapping efficiency of condensable gas in the reactor and transfer cold traps would result in a fraction of the condensable volatiles reaching the molecular sieve, from which they would not evolve for subsequent detection. To determine the trapping efficiency of condensables in the reactor traps and in the "U" trap, therefore, it is enough to perform a degradation experiment and determine the proportions of probe gas (in this case carbon dioxide) left in the reactor and in the "U" trap (desired) and transferred to the molecular sieve trap (not desired).

As already mentioned in this discussion, carbon dioxide is irreversibly bound to activated 5A molecular sieve at room temperature, and therefore cannot be removed for analysis by simple pumping. To study this effect we condensed measured aliquots of carbon dioxide onto the molecular sieve trap at -196°C , then measured the amount or proportion recoverable at room temperature. Our results, summarized in Table 4, indicate that small amounts of carbon dioxide are indeed irreversibly bound onto molecular sieve at room temperature under high vacuum conditions, but that good recovery could be had simply by subsequent heating of the sieve trap to 200°C .

TABLE 4 EFFICIENCY OF RECOVERY OF CARBON DIOXIDE FROM 5A MOLECULAR SIEVE AT ROOM TEMPERATURE

RUN #	mg CO ₂ ONTO SIEVE ² AT -196°C	mg CO ₂ RECOVERED FROM SIEVE ² AT ROOM TEMPERATURE AS MEASURED BY IR SPECTROSCOPY
1	0.17	<0.1
2	0.56	<0.1
3	0.79	<0.1
4	1.10	<0.1
5	7.80	<0.1*
*8.11MG RECOVERED BY HEATING TRAP TO 200°C		

Having determined that the proportions of carbon dioxide in the receiving traps could be properly determined, we were then in a position to determine the trapping efficiency in our reactor using that gas as a probe. A 50mg sample of ATS-G was heated in the reactor to 800°C under 220mg oxygen. Condensable volatile products were then trapped in the liquid nitrogen traps and noncondensable volatiles in the molecular sieve trap at the end of the experiment. The sieve trap was then warmed to room temperature and the noncondensable fraction was flushed to the pumps. The trap was then heated to 200°C and the carbon dioxide transferred to a calibrated gas phase infrared cell for analysis as described in an earlier communication⁽⁴⁾. By this method it was found that less than 0.1mg of carbon dioxide was transferred to the molecular sieve trap. Later experiments showed that a 50mg sample of polymer, under these conditions, produced an average of 20.2mg of carbon dioxide in this experiment, as measured by material recovered from the liquid nitrogen traps. The trapping efficiency for carbon dioxide in this experiment, was, therefore, shown to be greater than 99%.

10. Product Analysis

All four of the product fractions of oxidation, namely the condensable and noncondensable gas fractions, the oligomeric products, and the residue of degradation, could be isolated for subsequent analysis using this experiment. Individual cases are summarized below.

a. The Residue of Oxidation

Residues of oxidation were determined by simple gravimetry. The preweighed crucible was removed from the degradation tube at the end of the experiment and reweighed to determine residual sample weight. The percent residue was then determined as $(\text{Final Weight}/\text{Initial Weight}) \times 100$.

b. The Oligomeric Product Fraction of Oxidation

The sample crucible was removed from the degradation tube at the end of the experiment. The oligomeric products, which condensed onto the upper part of the tube near the cooling coils, were then rinsed from the reactor with chloroform into a small beaker for subsequent analysis by infrared spectroscopy.

c. The Condensable Volatile Product Fraction of Oxidation

Noncondensable products of oxidation were removed from the reactor, which was pumped to a high vacuum. Siphon tubes were inserted into the cold traps from which liquid nitrogen was sucked

using house vacuum. The condensable volatile products of oxidation were then evaporated into the TVA manifold, collected there, and subsequently analyzed by SATVA, gravimetry, quantitative gas phase infrared, and proton NMR spectroscopy.

The oxidation process produces large quantities of carbon dioxide which could not be properly analyzed in the calibrated infrared gas cell. For this reason, the gas cell was attached to the vacuum manifold through a calibrated gas expansion bulb, as depicted in Figure 27. Its principle of operation is quite simple. Condensable volatile products of oxidation are first condensed into the cold finger of the gas IR cell. The whole assembly is then isolated from the vacuum line, and the products warmed to room temperature. By the ideal gas law (which these materials obey due to the low pressures involved) the gas partitions between the two containers according to the ratio of their volumes. Knowing this ratio, from the quantity of CO_2 in the gas cell, as measured from band intensities such are reproduced in Figure 28, we can work out the total CO_2 produced in the degradation experiment.

A typical gas phase IR spectrum of the condensable volatile products of oxidation of ATS-G resin is shown in Figure 29. A typical proton NMR spectrum of the same material, is shown in Figure 30.

d. The Noncondensable Volatile Product Fraction of Oxidation

At the end of the experiment, noncondensable material was pumped into a 5A molecular sieve trap held for that purpose at

-196°C. The trap was warmed to room temperature, and evolved gas was transferred in 4 aliquotes to a gas phase infrared cell with molecular sieve, which had been previously calibrated for carbon monoxide and methane as previously outline⁽⁴⁾. A typical gas phase IR spectrum of one of these aliquots is show in Figure 31.

SECTION VI

OXIDATION OF ATS-G UNDER CLOSED SYSTEM CONDITIONS

Using the techniques developed in the previous section, we set out to tackle the problem of the mechanisms of oxidation of ATS resins under partially anaerobic conditions, and by so doing, produce data to perhaps answer the question of the nature of the primary oxidation step in such an experiment, and by inference, also within articles of macroscopic dimensions and composed of like materials, exposed to similar accelerated oxidations in the presence of a limited supply of oxygen.

We, first of all, recount a short list of simple analyses which were performed for this purpose on the four product fractions of oxidation of ATS polymers. We next explore the nature of the bulk oxidation reaction using predegraded resin, and finish with some simple arithmetic which appears to support the contention that the primary reaction of these thermally stable resins under conditions of accelerated decomposition in a limited supply of oxygen is thermal in nature.

1. SATVA of the Condensable Volatile Products of Oxidation to 800°C

Samples of precured ATS-G (50mg and 100mg) were oxidized to 800°C at a heating rate of 5°C/min in contact with 220mg oxygen as outlined in the previous section. The condensable volatile products of oxidation were then trapped in the vacuum line and separated for analysis by SATVA. Corresponding SATVA traces for the two polymer weights are reproduced in Figures 32 and 33, from which it can be seen that the product distribution of anaerobic degradation, as reproduced in Figure 3, is somewhat, but not completely, altered by the presence of a limited supply of oxygen. (Although the anaerobic experiment was performed to an end temperature of 1020°C, we can compare the two because condensable volatile products of thermal degradation are quantitatively produced only below 800°C under those conditions.)

If we directly compare SATVA traces from 100mg samples degraded under vacuum and in the presence of a small amount of oxygen, as illustrated in Figures 3 and 33, we can see that the yields of sulfur dioxide are similar, but that the yields of benzene and phenol are reduced, and that the yields of carbon dioxide and water are increased when oxygen is present. The obvious, and quite probably true, explanation for this effect, is that benzene and phenol are oxidized after formation to carbon dioxide and water. If we compare the SATVA traces from 50mg and 100mg samples of polymer which had been oxidized by oxygen gas, it can be seen that a proportionately larger fraction of benzene and

phenol are converted to carbon dioxide and water in the product distribution from the 50mg sample than in the corresponding distribution from the 100mg sample. From this comparison, it becomes obvious that the oxidation reaction proceeds more efficiently as the mass ratio of oxygen to polymer in the reactor increases.

2. Gravimetric Analysis of the Residues of Oxidation to 800°C

The percentage residues of degradation of ATS-G to 800°C in air, under helium, and in a high vacuum were measured, in most cases, simply by comparing "before and after" weights as (Before/After) x100. The sole exceptions were results from the TGA experiments performed under helium and in air, which were simply read from the dynamic weight loss curves. Residues of degradation are quoted in Table 5.

TABLE 5 RESIDUES OF THERMAL AND OXIDATIVE DEGRADATION OF ATS-G TO 800°C AT 5°C/MIN

EXPERIMENT	RESIDUE AS WEIGHT % OF THE CURED POLYMER
TVA (High Vacuum)	55.2
TGA Under Helium	57.6
50mg in Oxidation Reactor	58.5
100mg in Oxidation Reactor	59.4
TGA in Air	0.0

The most striking feature of this set of measurements is the similarity between all residue weights save that from the TGA

experiment performed in air. Similarities between weight loss experiments performed under helium and under vacuum were expected from previous work⁽⁴⁾. A discrepancy between those results and that from the TGA experiment performed in air was also expected, due to the operation of the high temperature bulk oxidation reaction which quantitatively volatilizes resin exposed to, what is to all extents and purposes, and unlimited supply of oxygen. More surprising, was the good agreement between weight loss experiments performed under inert conditions and in the oxidation reactor, from which it can be deduced that the bulk oxidation reaction is heavily suppressed under conditions where oxygen is present in small quantities only. Presumably, under these conditions, oxygen, at the temperatures at which the bulk oxidation reaction is operative, has been reduced below a level at which it can efficiently react with the sample, perhaps by reaction with volatile products of thermal degradation, as is suggested by the results of the SATVA experiments.

3. Oligomer Product Analysis

A small quantity of oligomer was recovered from experiments in which 100mg samples of ATS-G were degraded to 800°C in the oxidation reactor. Material collected from several experiments was combined to obtain the infrared spectrum shown in Figure 34, which, on comparison with that of the oligomeric product fraction of thermal degradation of the same polymer, as show in figure 35,

appears similar, but contains absorption bands which suggest the presence of more saturated material and some carbonyls in the oxidized material, both of whom may be intermediates of the oxidation process. It was interesting to note that no oligomeric products were recovered from the 50mg samples which were oxidized under the same conditions. Oligomeric products of the thermal degradation of ATS-G, which are formed predominantly in the temperature range 400-600°C, must, therefore, be completely oxidized in the gas phase to lower molecular weight products when oxygen is more freely available for reaction with the polymer, as is encountered with smaller samples in contact with the same amount of gas.

4. Quantitative Volatile Product Distributions of Oxidation to 800°C

The volatile products of oxidation to 800°C of ATS-G were analyzed quantitatively by methods outlined in Section V of this discussion. Average product distributions from 50mg and 100mg samples are illustrated in Table 6 and 7 respectively.

Degradation experiments performed in the presence of oxygen differ from those performed in the absence of oxygen in that the combined weight of volatile products plus residue is not equal to the initial sample weight, because of reactions of the polymer and its degradation products with oxygen. For this reason, the volatile products of oxidation were monitored also by their carbon content as well as total mass, for comparison with the products of

thermal degradation of the resin (from Table 1), as is shown in Table 8.

TABLE 6 PRODUCT DISTRIBUTION OF CLOSED SYSTEM OXIDATION TO 800°C OF 50mg ATS-G

PRODUCT	PRODUCT WEIGHT (mg)	WEIGHT VOLATILIZED CARBON/50mg CURED POLYMER (mg)
H ₂	Negligible	0.0
CH ₄	0.5	0.4
CO ¹	11.0	4.7
CO ₂	20.2	5.5
SO ₂	5.1	0.0
Benzene	Negligible	0.0
H ₂ O	11.8	0.0
Phenol	Negligible	0.0
COS	0.6	0.1
<u>TOTAL</u>	<u>49.2</u>	<u>10.7</u>

TABLE 7 PRODUCT DISTRIBUTION OF CLOSED SYSTEM OXIDATION TO 800°C OF 100mg ATS-G

PRODUCT	PRODUCT WEIGHT (mg)	WEIGHT VOLATILIZED CARBON/100mg CURED POLYMER (mg)
H ₂	Negligible	0.0
CH ₄	4.6	0.5
CO ¹	20.1	8.6
CO ₂	11.6	3.2
SO ₂	12.6	0.0
Benzene	1.3	1.2
H ₂ O	18.3	0.0
Phenol	2.4	1.9
COS	1.3	0.3
<u>TOTAL</u>	<u>72.2</u>	<u>18.7</u>

TABLE 8 WT % CARBON VOLATILIZED FROM ATS-G DEGRADED UNDER VACUUM AND IN OXYGEN

CONDITIONS OF EXPERIMENT	WT% TOTAL VOLATILES	WT% VOLATILIZED CARBON
TVA (Vacuum)	47.9	21.7
50mg in Reactor	98.4	21.4
100mg in Reactor	72.2	18.7

Similarities between the volatile product yields expressed in terms of carbon content appear rather compelling evidence in support of the contention that such products of accelerated oxidations of the polymer under conditions of limited oxygen availability, arise, in the main, from secondary gas phase oxidations of corresponding products of thermal degradation. The relatively lower yield of carbon from a 100mg sample of the resin upon degradation in the reactor, is probably a direct result of inefficient oxidations of the oligomeric product fraction of thermal degradation. (Remember that carbon in the oligomeric product fraction of thermal degradation was counted in that product distribution, that no oligomeric products were detected in the product distribution of oxidation of a 50mg sample of polymer in the reactor, and that some oligomeric products of oxidation were detected in the oxidative product distribution from a 100mg sample in the reactor, but those products could not be quantified for addition to the total carbon count.) This situation is concisely illustrated by comparing the carbon dioxide to carbon monoxide

product ratios of oxidation of 50mg and 100mg samples of resin in the reactor. The results, illustrated in Figure 9, show quite concisely that the carbon dioxide to carbon monoxide ratio, which may be thought of as an index to the efficiency of the oxidation reaction, supports the contention that the 50mg samples are more efficiently oxidized than the 100mg samples.

TABLE 9 CARBON DIOXIDE/CARBON MONOXIDE PRODUCT RATIOS OF OXIDATION TO 800°C OF ATS-G

SAMPLE SIZE (mg)	MOLE RATIO CO ₂ /CO (EFFICIENCY OF OXIDATION)
100	0.4
50	1.2

5. Oxidation of Thermally Degraded ATS-G

Due to the fact that oxygen is efficiently consumed by reaction with the volatile products of thermal degradation of ATS-G in the reactor, it is not possible to obtain a product distribution from the high temperature bulk oxidation by directly oxidizing the base resin. However, this process may be conveniently studied in isolation by oxidizing predegraded ATS-G. In brief, a sample (54.2mg) of precured ATS-G was heated in the oxidation reactor under high vacuum conditions to 700°C at 5°C/min to drive off the products of thermal degradation. The residue of degradation (28.3mg of almost pure carbon), was reheated to 700°C at 5°C/min in the presence of 220mg oxygen in the usual fashion, to leave a

residue of oxidation (21.4mg). The volatile products of the bulk oxidation reaction were collected and analyzed by SATVA as shown in Figure 36, and by quantitative gas phase infrared spectroscopy. If we consider that the Pirani gauge output is decidedly nonlinear and much compressed towards higher pressures, it can be seen from the SATVA trace that, as expected, carbon dioxide and water constitute the bulk of the product distribution of oxidation of this material. A quantitative product distribution for this process is shown in Table 10, from which it can be seen that 6.7mg of volatile carbon is produced in a process which removes 6.9mg of material from the sample. The discrepancy between the two may have been produced by errors in the experiment, or may give some indication of the quantity of hydrogen in the residue which reacts with oxygen to form water. Oxygen is, therefore, shown to volatilize the residue of vacuum degradation of ATS-G by removing carbon as carbon monoxide and carbon dioxide, and hydrogen as water, in quantities which are presumably dictated by the availability of oxygen to the polymer.

TABLE 10 A PRODUCT DISTRIBUTION FOR THE HIGH TEMPERATURE BULK OXIDATION REACTION OF ATS-G

PRODUCT	WT PRODUCT	WT CARBON IN THE PRODUCT (mg)
CO	4.4	1.9
CO ₂	17.7	4.8
Benzene	Negligible	Negligible
<u>TOTAL</u>	<u>22.1</u>	<u>6.7</u>

6. Translation to a Composite Environment

ATS-G is under evaluation primarily as a resin adhesive for the formulation of high performance composites for the aerospace industry. As such, most resin, by virtue of the low surface to volume ratio of a composite piece of finite size, if subjected to flash thermolysis in air, would do so under conditions of restricted oxygen access, such as is encountered with the oxidation reactor. Of course, low temperature, long term oxidations of the resin will be promoted by diffusion of oxygen through the resin matrix, and, in the time frame of the experiment, be relatively free of diffusion controls. In contrast, higher temperature flash oxidations of the bulk resin in an intact composite piece, must be powered by immediately available oxygen, presumably contained in adjacent voids or other structural irregularities.

We have shown in this series of experiments that the high temperature bulk oxidation reaction of a 60-micron-thick, 50mg sample of ATS-G resin, in contact with 220mg oxygen, is effectively suppressed under closed system conditions in the oxidation reactor. Using this fact, it becomes possible to estimate a relative (gas containing) void/resin volume ratio which approximates the purely artificial conditions within the reactor. We will subsequently assume that the bulk oxidation reaction is effectively suppressed at void/polymer ratios below this value. Of course we do not possess any information which would suggest behaviour at such ratios in excess of this value.

We will, first of all, state some facts. For example, the average thickness of a composite article will be significantly greater than the 60-micron samples used here. Problems of gas diffusion to the active site (the degrading polymer) will, therefore slow down the process of oxidation with respect to samples examined in the reactor. In a similar vein, nitrogen, from air in the composite, and the volatile products of gas phase oxidations such as carbon monoxide, carbon dioxide, and water, will not be efficiently removed from that composite, and will hamper the inward diffusion of fresh oxygen, to further slow down the process of oxidation.

We will next make some assumptions. First of all, we will assume that any voids within the composite contain unmodified air with about 20% oxygen content, initially at 1 atmosphere pressure at room temperature. We next assume that air is not lost from the composite by gas expansion through the void system as the composite is heated quickly to degradation temperatures. Finally, we assume that the density of ATS-G resin is approximately 1g/cc, although a figure of about 1.4g/cc would probably be more accurate.

The "Calculation"

1. Volume of 220mg O₂ at STP

$$0.220\text{g O}_2 = 6.9 \times 10^{-3}\text{M O}_2 = 3.44 \times 10^{-2}\text{M of Air}$$

Volume at STP from the ideal gas law = 840cc

2. Volume of 50mg ATS-G at STP

50mg resin at a density of 1g/cc = 0.05cc

3. Void (Gas Volume)/Polymer Ratio at STP

Ratio = 16800/1 (an impossible figure for a structural composite)

The volume ratio calculated above (16800/1) suggests that the primary processes of flash degradation within an article of any size and composed of ATS-G must be thermal in nature, thus validating the use of programmed TGA as a tool for the rapid evaluation of the stability of these materials. We are now also in a position to examine a worst case scenario - for example, if we instead, postulated that the composite contained pure oxygen at a pressure to 10 atmospheres carried through from autoclave manufacture, the calculated void to polymer ratio to match the conditions met in the oxidation reactor would still exceed 300/1 - a figure more applicable to a blown polyurethane foam than to a structural composite. The high temperature bulk oxidation reaction of ATS-G resin is, therefore, probably efficiently suppressed while that composite retains its structural integrity.

SECTION VII

CONCLUSIONS

We first found that ATS-G and its component fractions possess similar stabilities to high temperature oxidation as measured by

the programmed TGA experiment, and that the impurities in ATS-G resin do not appear to appreciably lower its stability below that of pure ATS monomer or dimer. We also found that all ATS polymers are completely volatilized in TGA experiments under air by what appears to be a two step process. The first stage, beginning at about 400°C, closely parallels, but is not identical to, the corresponding weight loss reaction operative in this temperature interval in vacuum or under inert atmosphere. The second process begins at about the same temperature interval at which the first thermal process ends and completely volatilized the remainder of the sample.

We also found that oxygen is not incorporated into the polymerizing polyene chains to any significant extent (by weight) during resin cure. Nonetheless, those polymers which had been cured in the absence of oxygen were shown to be measurably more stable to subsequent high temperature oxidations than those cured in air. We can only assume that oxygen modifies the polyene network in some way during its formation, to somehow reduce high temperature stability, perhaps by interfering with the ability of the polyene to aromatize at high temperatures. More work is clearly needed to clarify possible mechanisms of interaction of the growing polyene with oxygen.

A comparison of TGA curves in air of the ATS polymers, made us wonder if the temperature profile of the high temperature bulk oxidation reaction matched its chemical stability (in other words, did the process occur in that temperature interval because the

structure became unstable at those temperatures, or was the process artificially delayed to higher temperatures by the first process of degradation). This question was easily solved by oxidizing prethermolysed resin, which, without the delay imposed by the first process of degradation, reproducibly oxidized at much lower temperatures, thus proving, in some way, that the first process of degradation delayed the onset of the bulk oxidation reaction.

(Subsequent experiments in the oxidation reactor confirmed that gas phase oxidation of the products of the first process of thermal degradation can consume significant amounts of oxygen to perhaps reduce its level in the reactor below that which could support the bulk oxidation reaction.)

A reactor was designed and built to subject polymers and resin to accelerated high temperature oxidative degradation under partially anaerobic conditions. Analytical protocols for the subsequent isolation of all four product fractions of oxidation were then developed and tested in operation. Using this experiment, it was shown that volatiles produced in the first stage of thermal degradation of a 50mg sample of precured ATS-G in contact with 220mg of oxygen, are efficiently oxidized in the gas phase to carbon monoxide, carbon dioxide, and water, in a process which lowers the oxygen level in the reactor below that which can efficiently support the higher temperature bulk oxidation reaction. When isolated, by oxidizing predegraded ATS-G in the reactor, the high temperature bulk oxidation reaction was shown to volatilize the residue of almost pure carbon, with some hydrogen, to carbon

monoxide, carbon dioxide, and water, in proportions which are determined by the availability of oxygen in the reactor.

With reference to the previous conclusion, some simple calculations were used to confirm that the initial mechanisms of decomposition of most resins of this type, in a part of finite size, and subjected to flash pyrolysis in air, must be thermal in nature, thus validating the use of programmed TGA under inert gas as a tool for the rapid evaluation of the stability of such resins, and that oxidative degradation of the bulk resin under accelerated conditions is unlikely while the part retains structural integrity.

REFERENCES

1. J. J. Harrison and C. M. Selwitz, AFWAL-TR-79-4183.
2. C. C. Kuo and C. Y-C Lee, AFWAL-TR-82-4037.
3. I. J. Goldfarb and W. T. K. Stevenson, AFWAL-TR-83-4011.
4. W. T. K. Stevenson, I. J. Goldfarb, and E. J. Soloski, AFWAL-TR- (in press).
5. S. Amdura, A. T. Y. Cheng, C. J. Wong, P. Ehrlich, and R. D. Allendoerfer, J. Polym. Sci., Polym. Chem. Ed., 16, 407 (1978).
6. G. Odian, "Principles of Polymerization", McGraw-Hill Inc., NY (1970).
7. D. W. Breck, W. G. Eversol, R. M. Milton, T. B. Reed and T. L. Thomas, J. Am. Chem. Soc., 78, 5963 (1956).
8. C. V. G. Nair and P. Vijendran, Vacuum, 27 (1), 549 (1977).

"FIGURES"

KEY

— Material Volatile at 0°C

- - - Material Volatile at -75°C

xxxx Material Volatile at -196°C

- . - . H₂

Heating Rate 5°C/min

Sample Size 101 mg

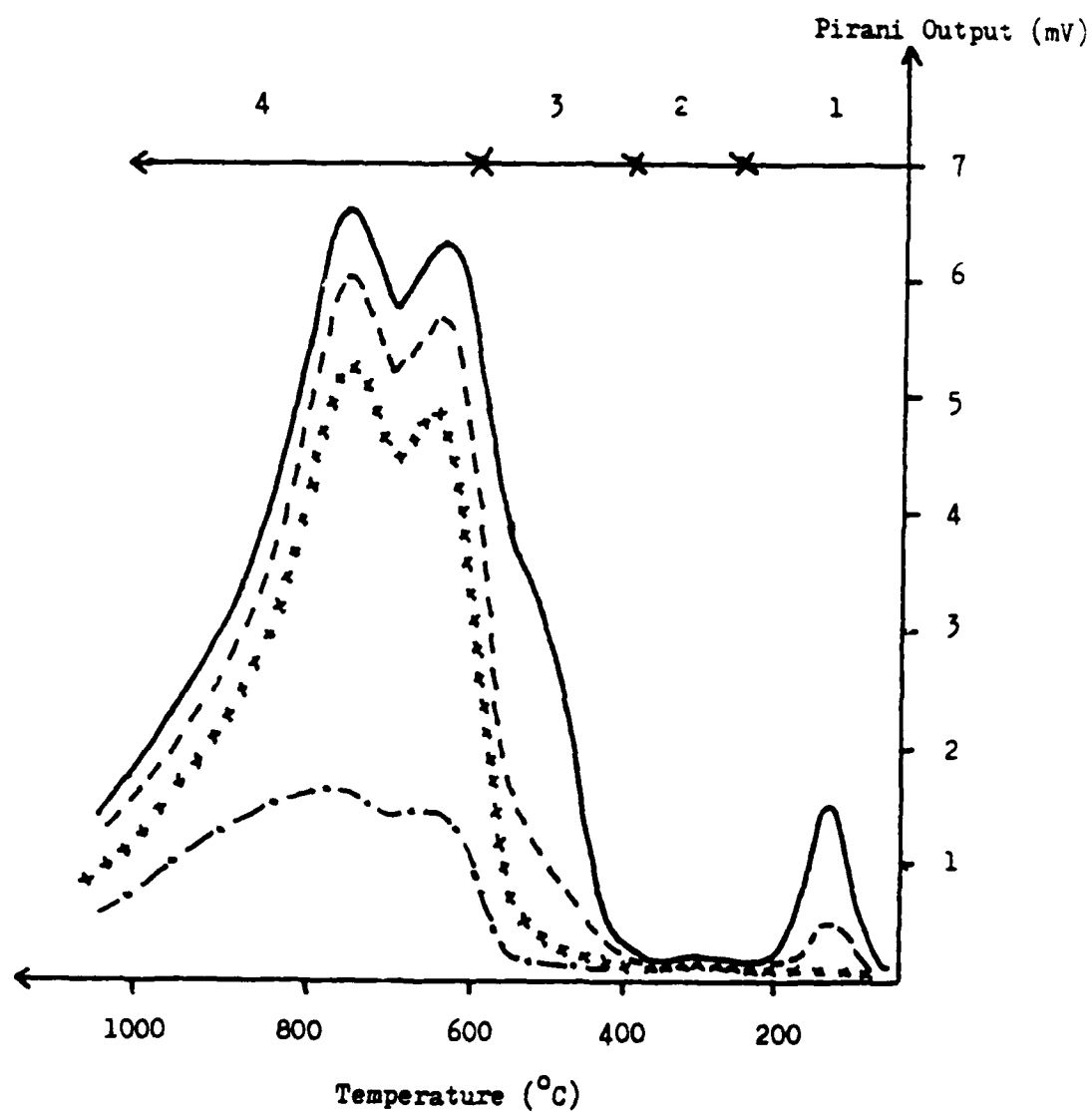


FIGURE 1 TVA TO 1020°C OF UNCURED ATS-G

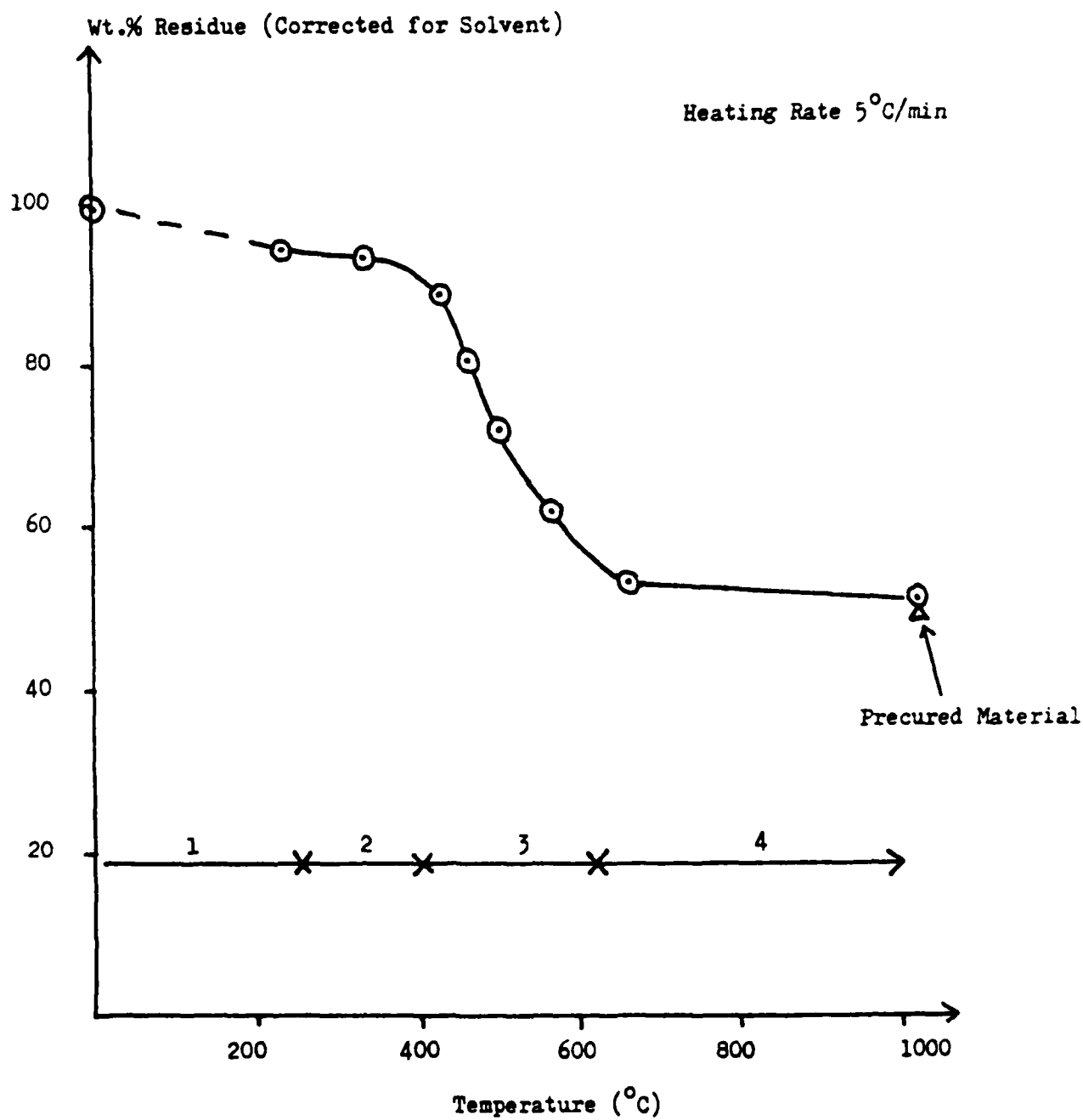


FIGURE 2 Wt. % RESIDUE OF VACUUM DEGRADATION OF UNCURED ATS-G

Sample Size 104 mg

KEY

- - - (-) Thermocouple Output (Trap Temperature)

— Pirani Output (Pressure)

1 CO_2, COS

2 SO_2

3 Benzene

4 Water

5 Phenol

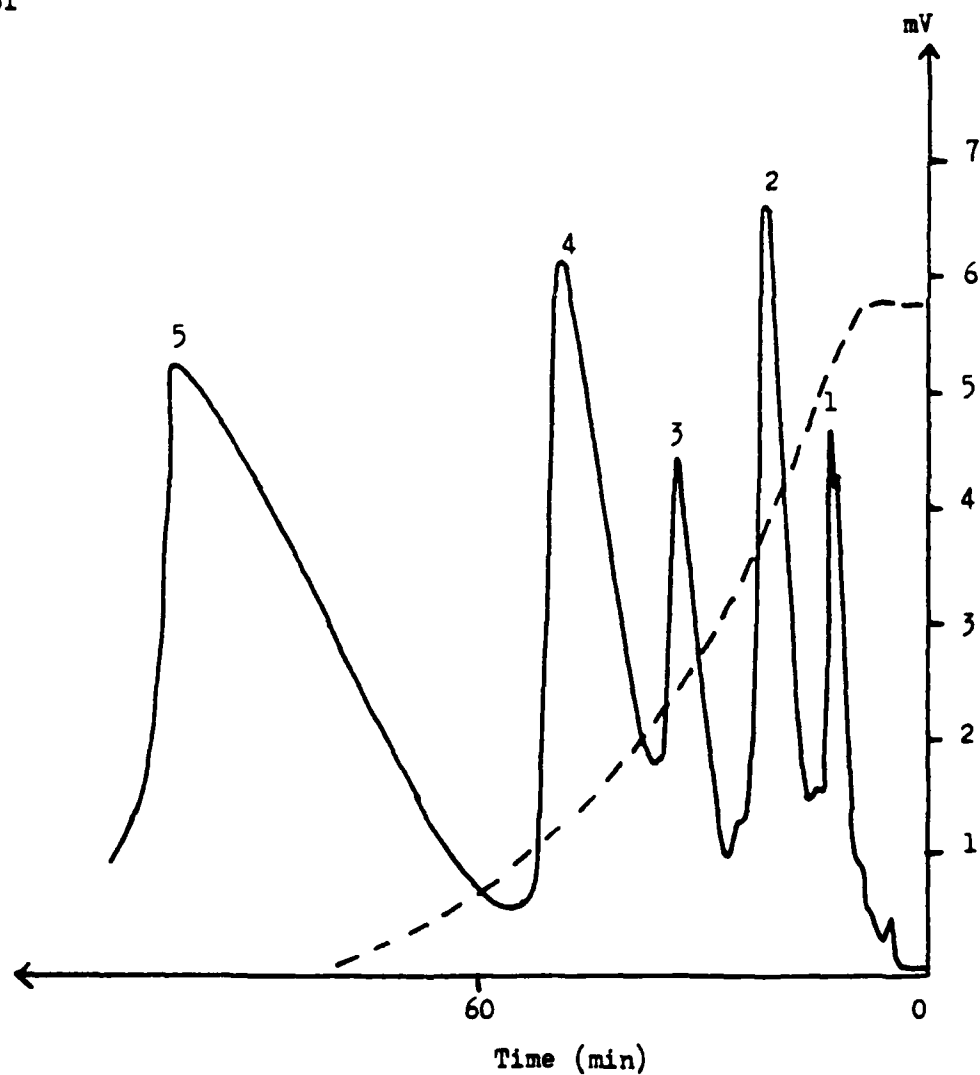


FIGURE 3 SATVA OF CONDENSABLE VOLATILE PRODUCTS OF THERMAL DEGRADATION TO 1020°C OF PRECURED ATS-G

Heating Rate 5°C/min

— Air, Sample Size 12.70 mg

-- Helium, Sample Size 10.60 mg

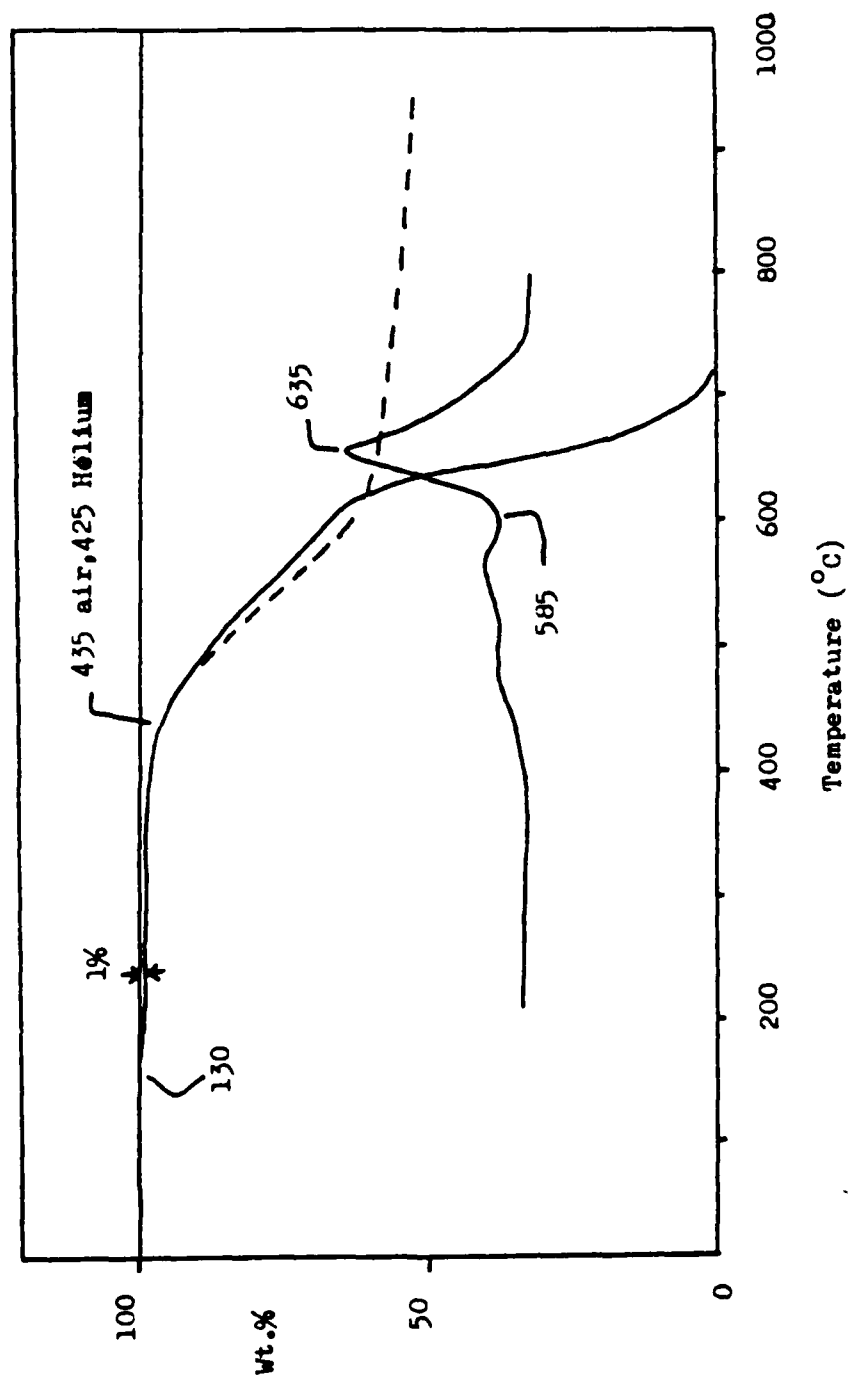


FIGURE 4 TGA OF ATS-G IN AIR AND UNDER HELIUM

Heating Rate 5 °C/min

— Air, Sample Size 16.85 mg

- - - Helium, Sample Size 12.15 mg

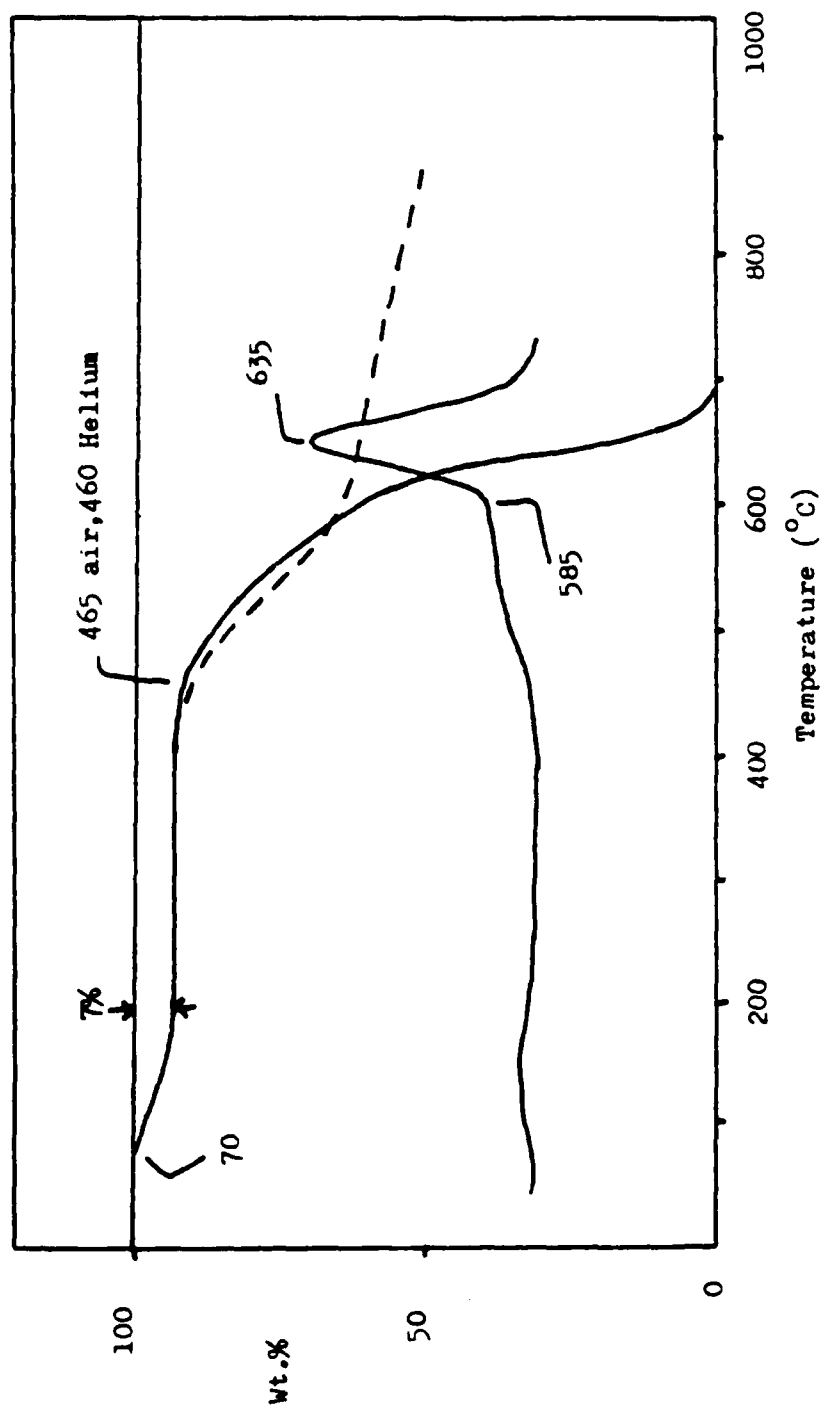


FIGURE 5 TGA OF ATS MONOMER IN AIR AND UNDER HELIUM

Heating Rate 5 °C/min

— Air, Sample Size 11.55 mg

- - - Helium, Sample Size 12.00 mg

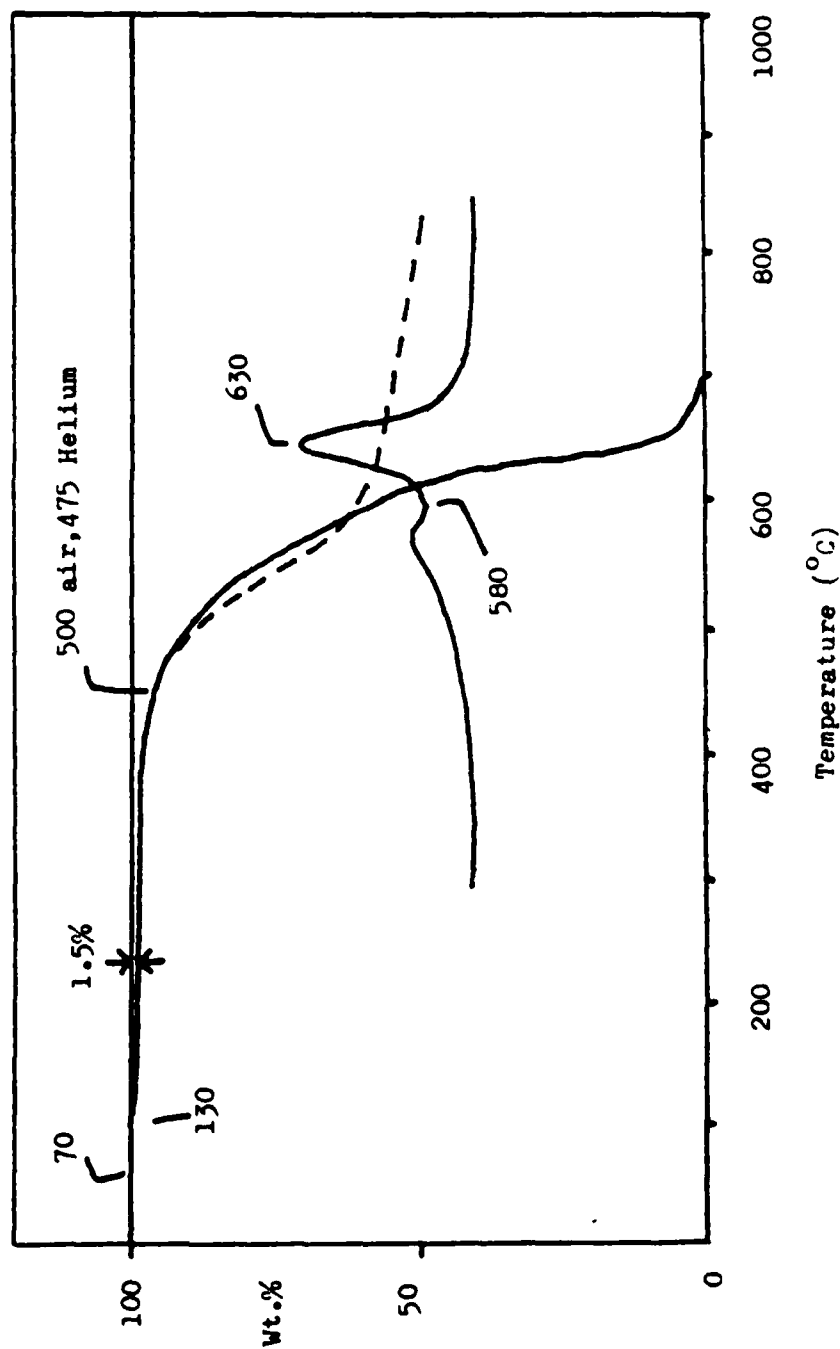


FIGURE 6 TGA OF ATS DIMER IN AIR AND UNDER HELIUM

Heating Rate 5°C/min

— Air, Sample Size 10.30 mg

- - - Helium, Sample Size 13.50 mg

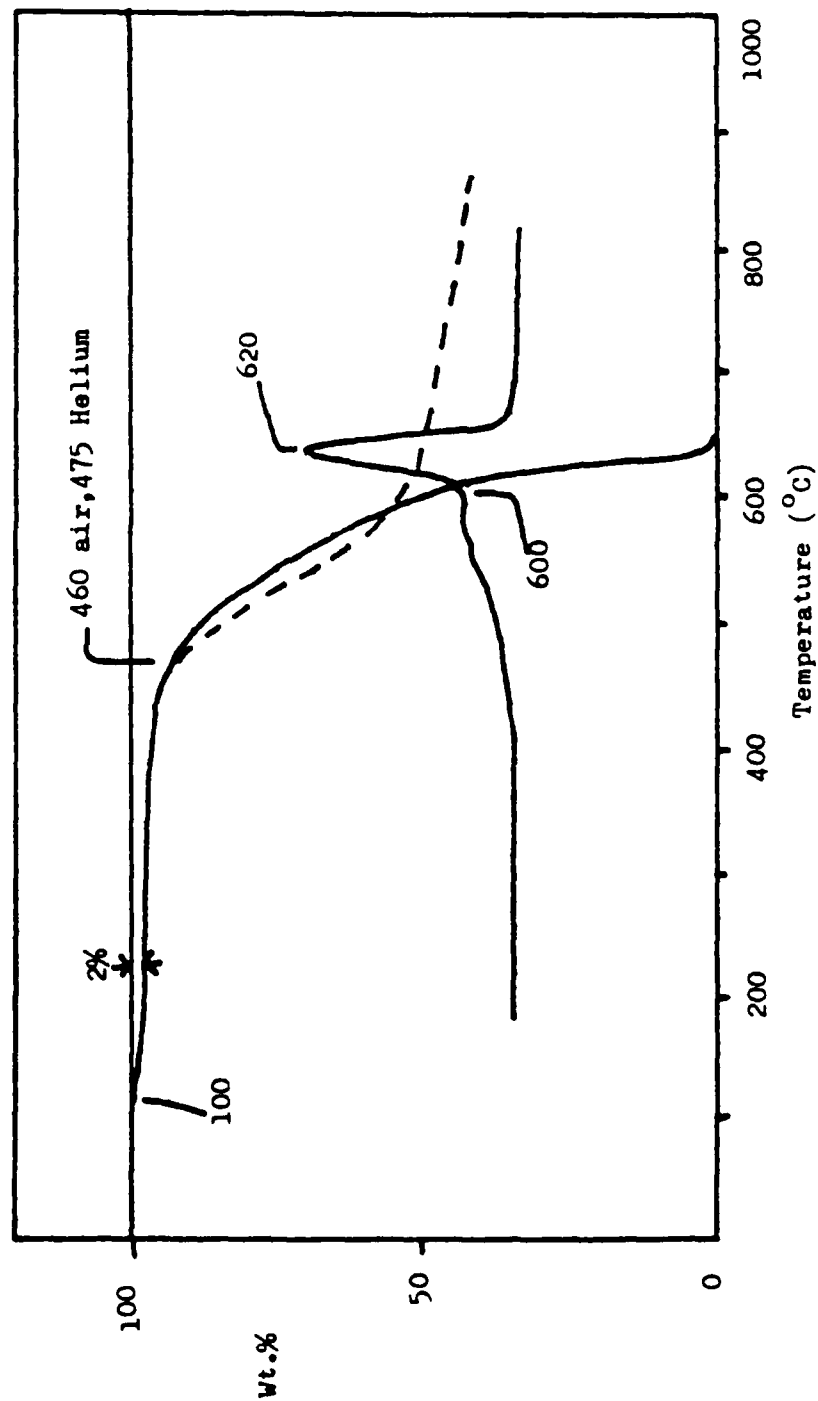


FIGURE 7 TGA OF ATS TRIMER IN AIR AND UNDER HELIUM

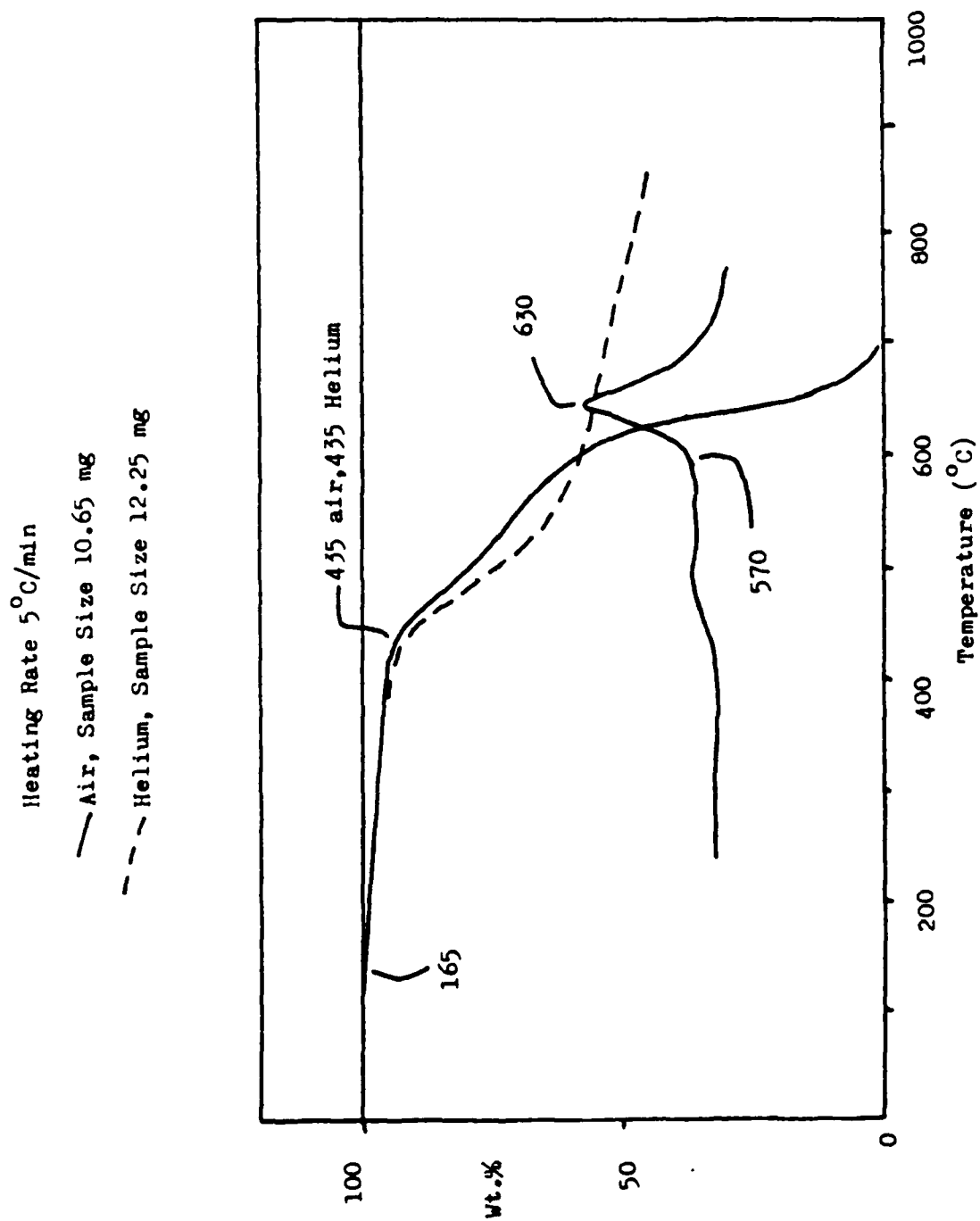


FIGURE 8 TGA OF F4 IN AIR AND UNDER HELIUM

Heating Rate 5°C/min

— Air, Sample Size 11.45 mg

-- Helium, Sample Size 11.10 mg

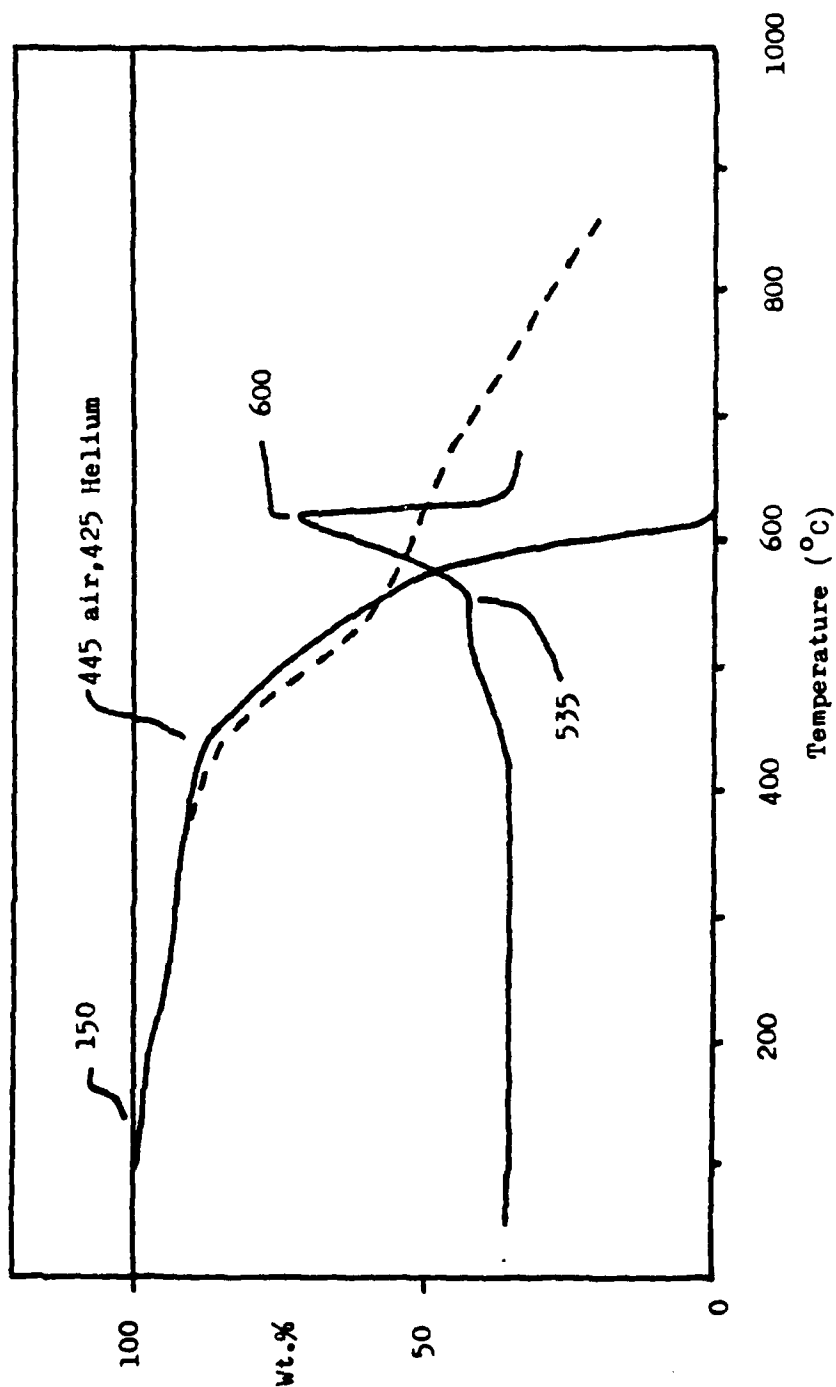


FIGURE 9 TGA OF F5 IN AIR AND UNDER HELIUM

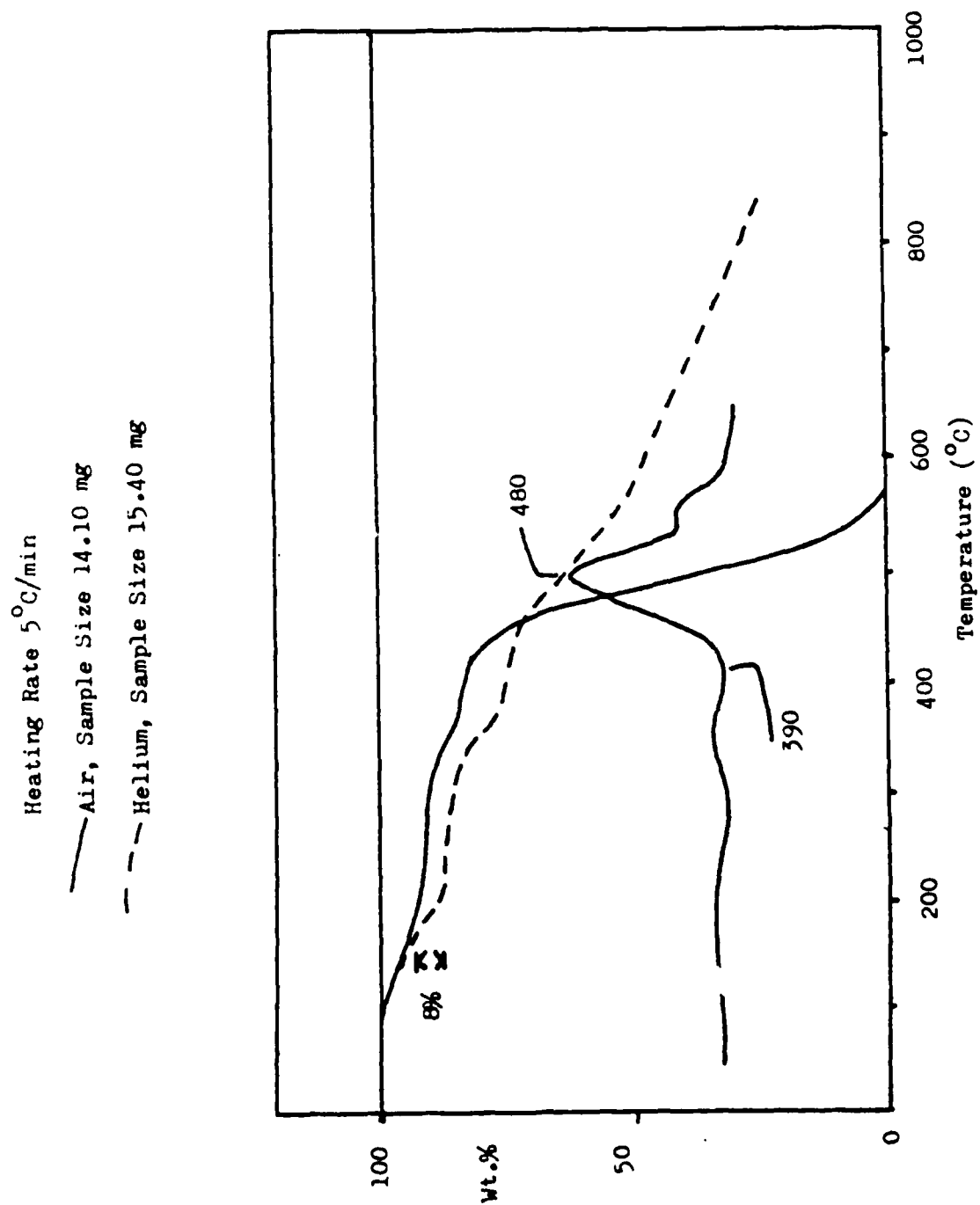


FIGURE 10 TGA OF F7 IN AIR AND UNDER HELIUM

KEY

— ATS-G

- - Mono ATS (F1)

+ x x x DI ATS (F2)

.... Tri ATS (F3)

. - - - F4

+ - - - + F5

Heating Rate 5°C/min

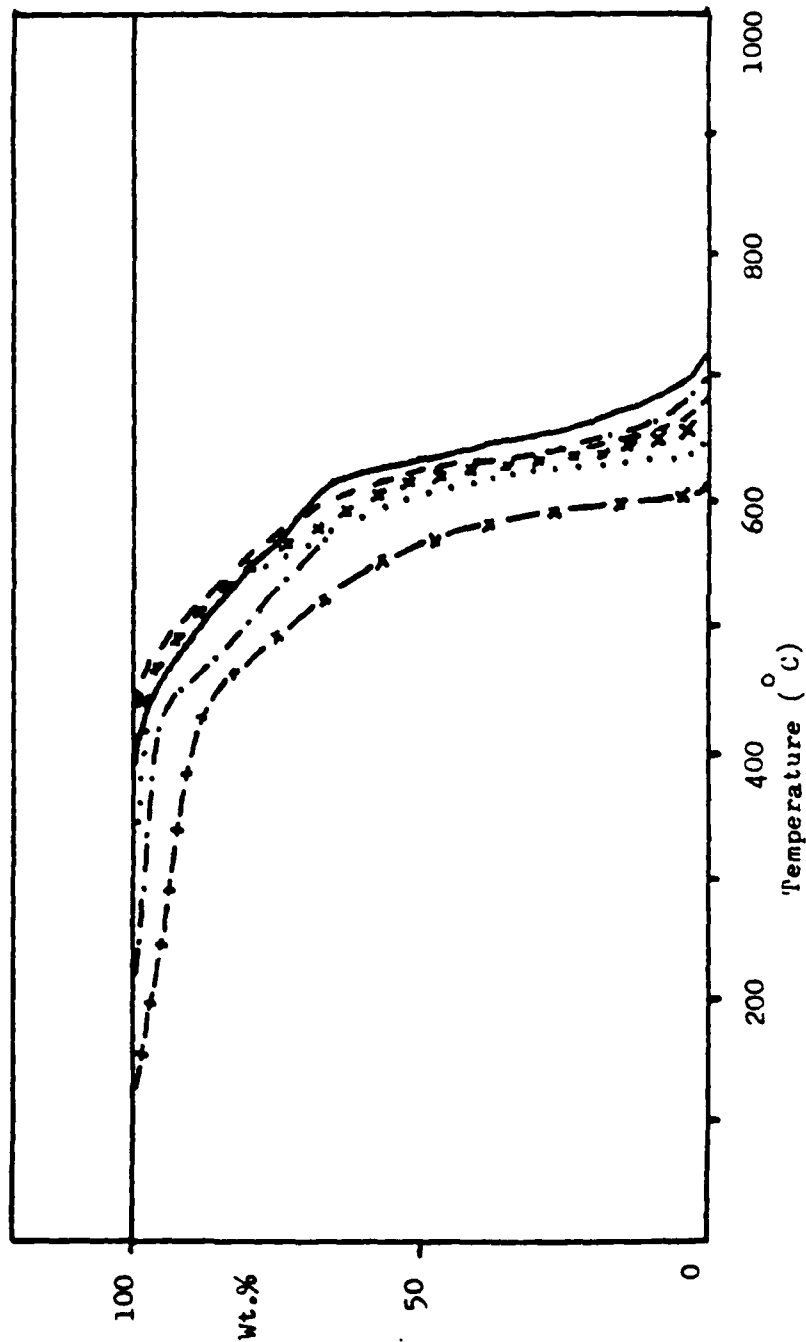


FIGURE 11 A COMPARISON BETWEEN SOLVENT COMPENSATED TGA CURVES IN AIR FOR UNCURED
ATS-G AND ITS COMPONENTS

Heating Rate 5°C/min

— Precured To 234°C At 5°C/min Under Vacuum, Sample Size 10.70 mg (Rate

Max. Of Oxidation - 640°C)

- - - Uncured, Solvent Compensated, Sample Size 12.70 mg (Rate Max. Of Oxidation - 635°C)

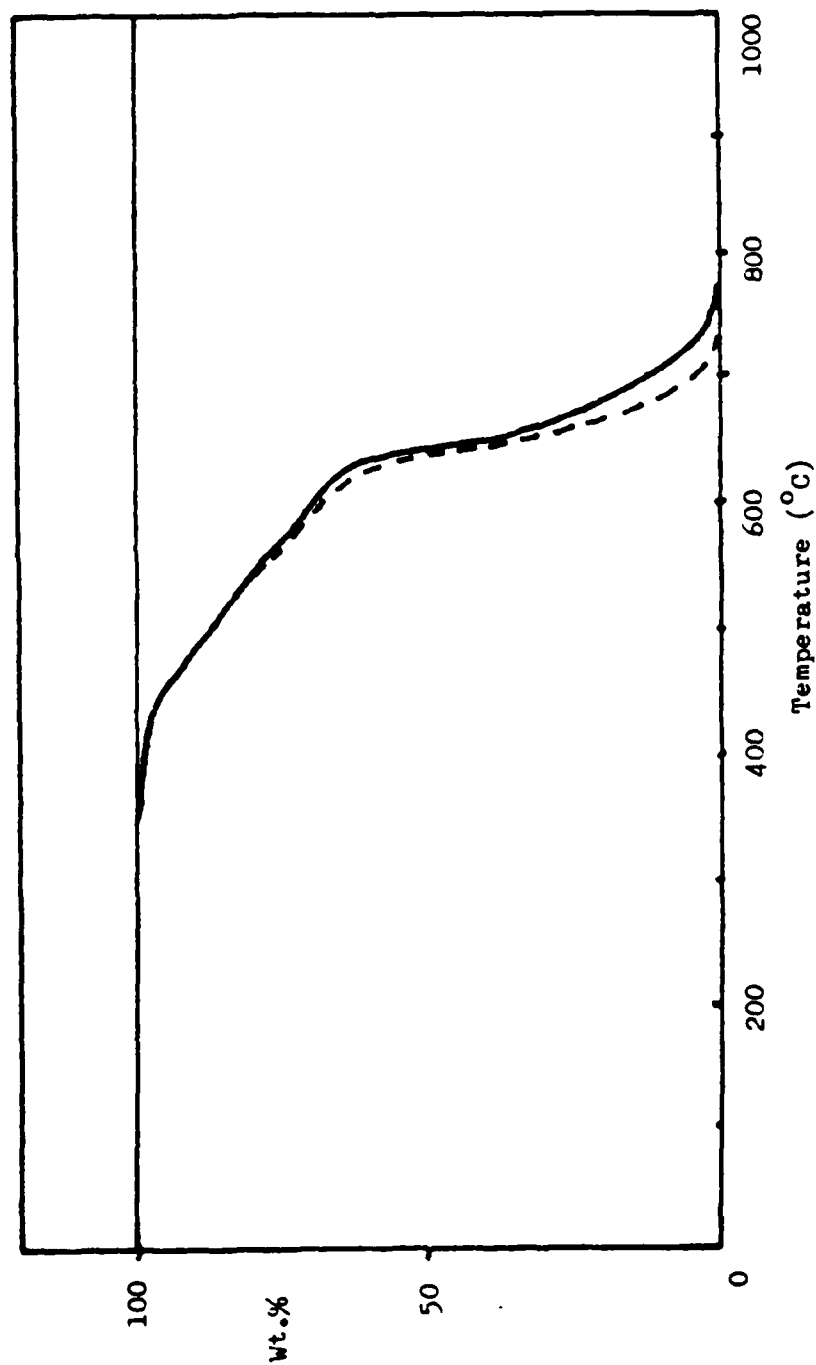


FIGURE 12 TGA IN AIR OF PRECURED AND UNCURED ATS-G

Heating Rate 5°C/min

- Precured To 234°C At 5°C/min Under Vacuum, Sample Size 11.85 mg (Rate Max. Of Oxidation - 640°C)
- - - Uncured, Solvent Compensated, Sample Size 16.85 mg (Rate Max. Of Oxidation - 635°C)

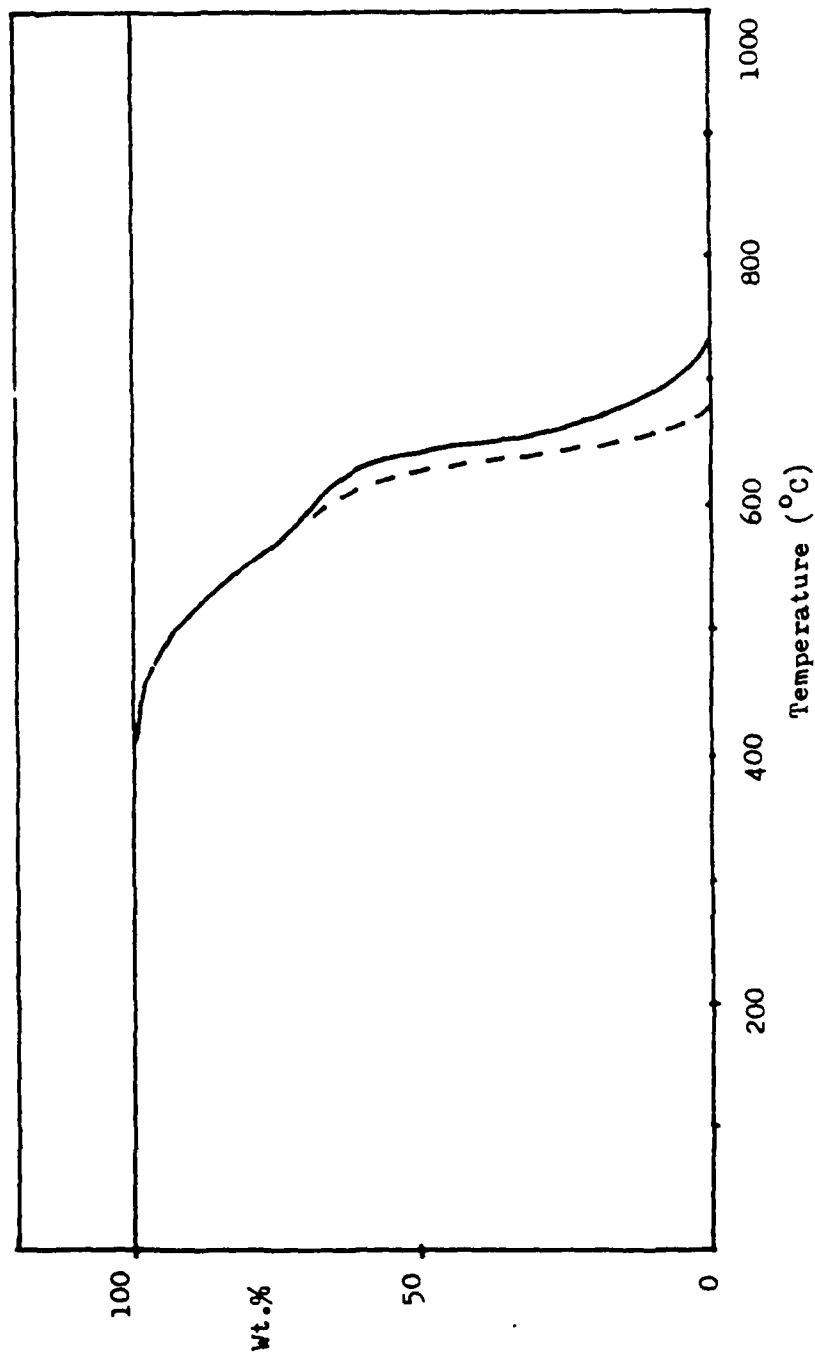


FIGURE 13 TGA IN AIR OF PRECURED AND UNCURED ATS MONOMER

Heating Rate 5°C/min

— Precured To 234°C At 5°C/min Under Vacuum, Sample Size 11.60 mg (Rate Max. Of

Oxidation - 635°C)

- - - Uncured, Solvent Compensated, Sample Size 11.55 mg (Rate Max. Of Oxidation - 630°C)

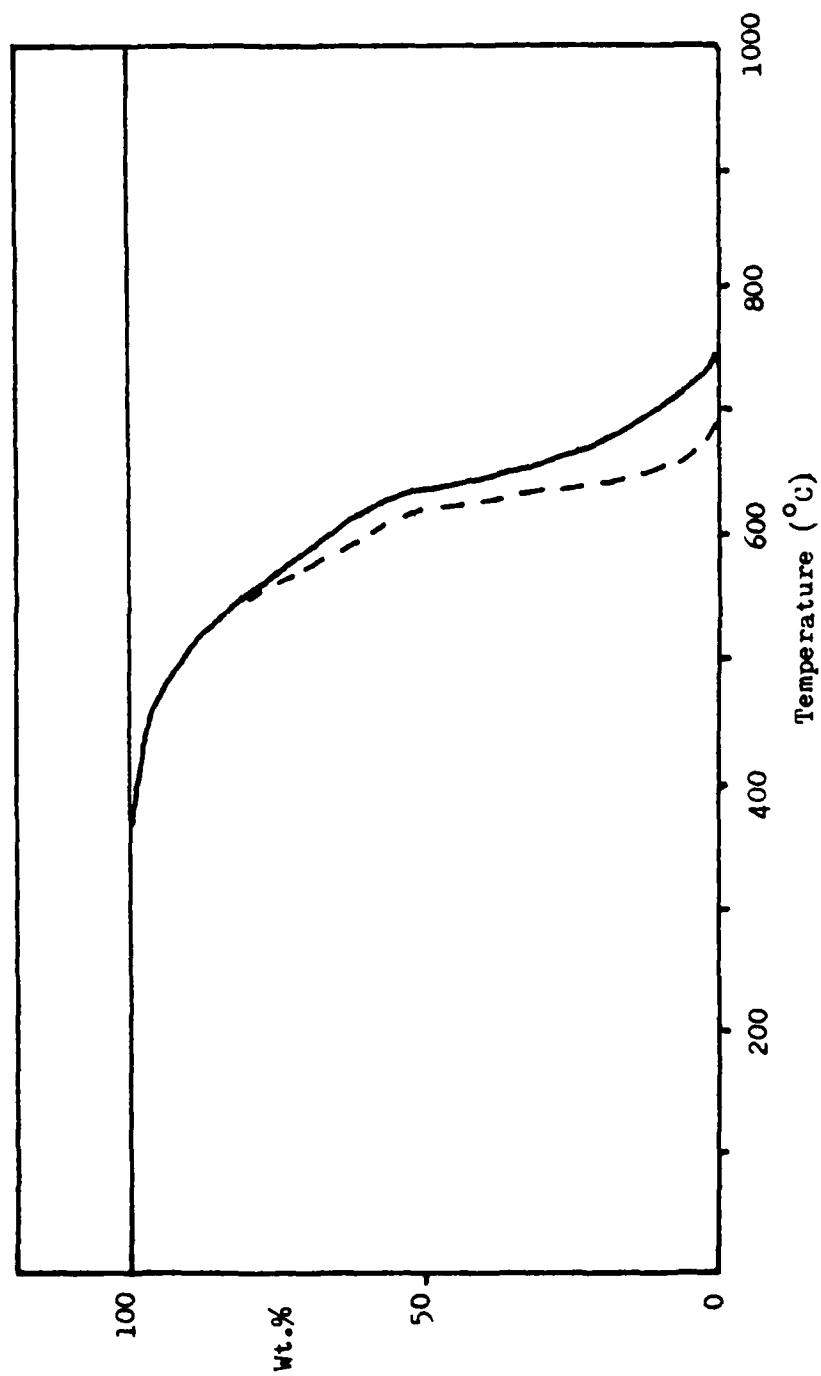


FIGURE 14 TGA IN AIR OF PRECURED AND UNCURED ATS DIMER

Heating Rate 5 °C/min

— Precured To 254 °C At 5 °C/min Under Vacuum, Sample Size 11.80 mg (Rate Max. Of

Oxidation - 635 °C)

- - - Uncured, Solvent Compensated, Sample Size 10.30 mg (Rate Max. Of Oxidation - 620 °C)

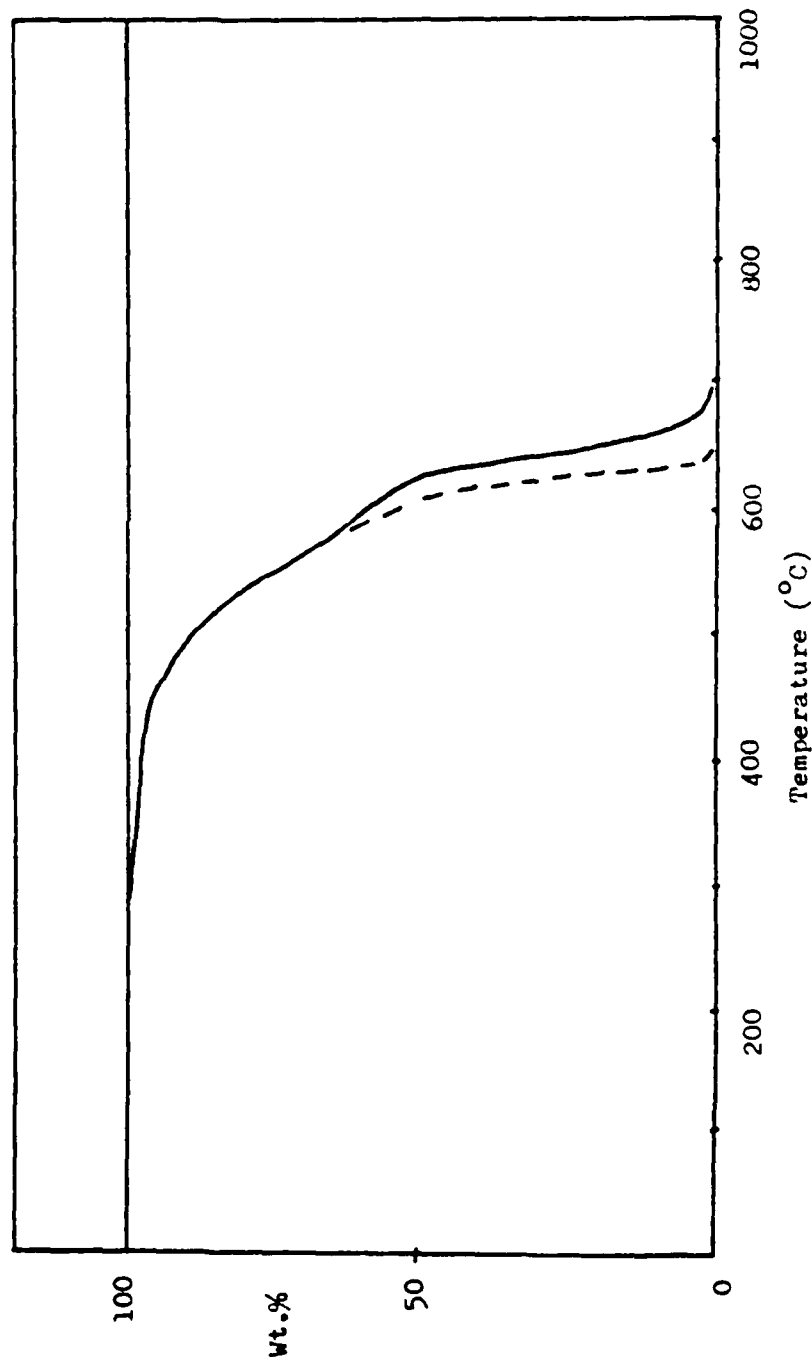


FIGURE 15 TGA IN AIR OF PRECURED AND UNCURED ATS TRIMER

KEY

— ATS-G

- - - Mono ATS (F1)

+ + + DI ATS (F2)

..... Tri ATS (F3)

Heating Rate 5°C/min

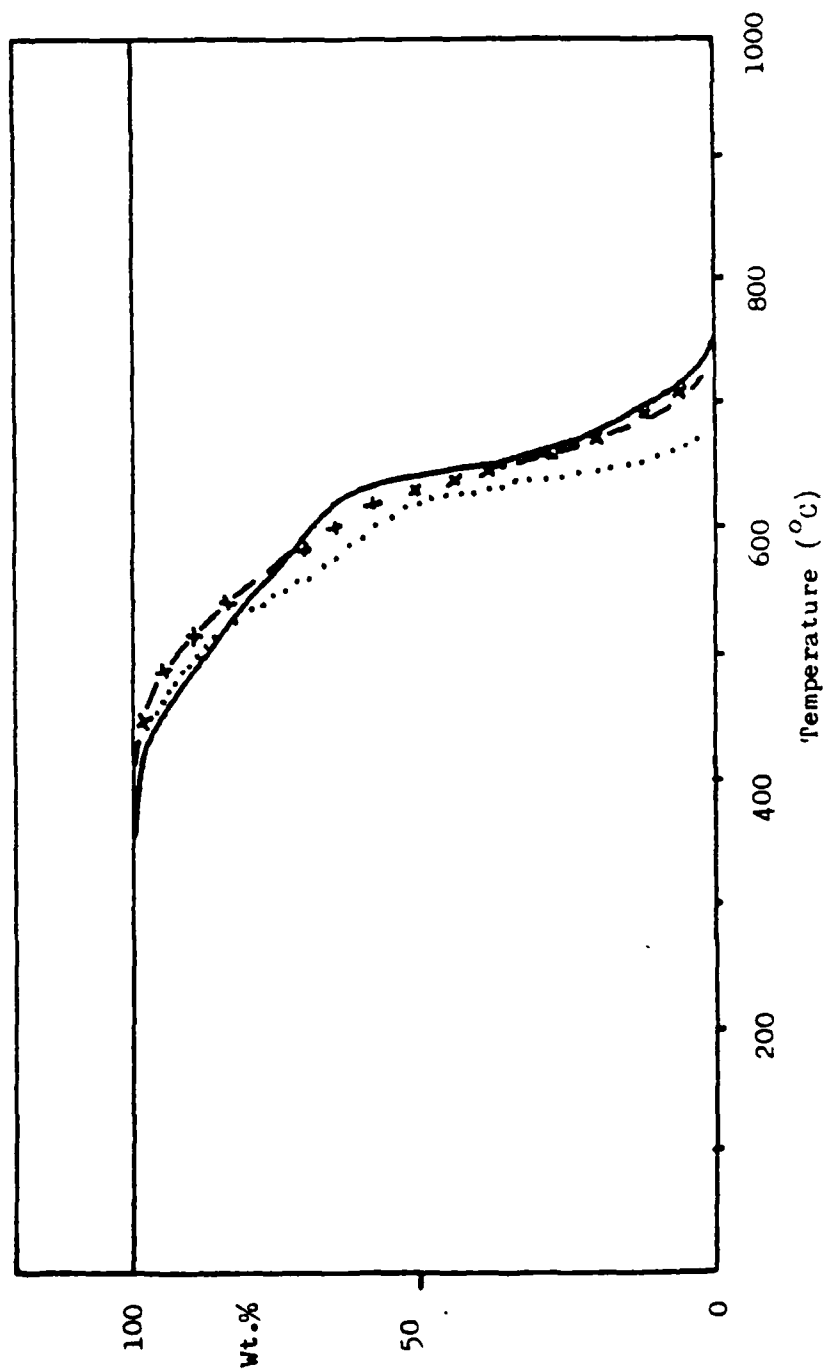


FIGURE 16 A COMPARISON BETWEEN TGA CURVES IN AIR FOR PRECURED ATS-G AND ITS COMPONENT FRACTIONS

Heating Rate 5°C/min

Sample Size 12.20 mg

-- Helium

— Air

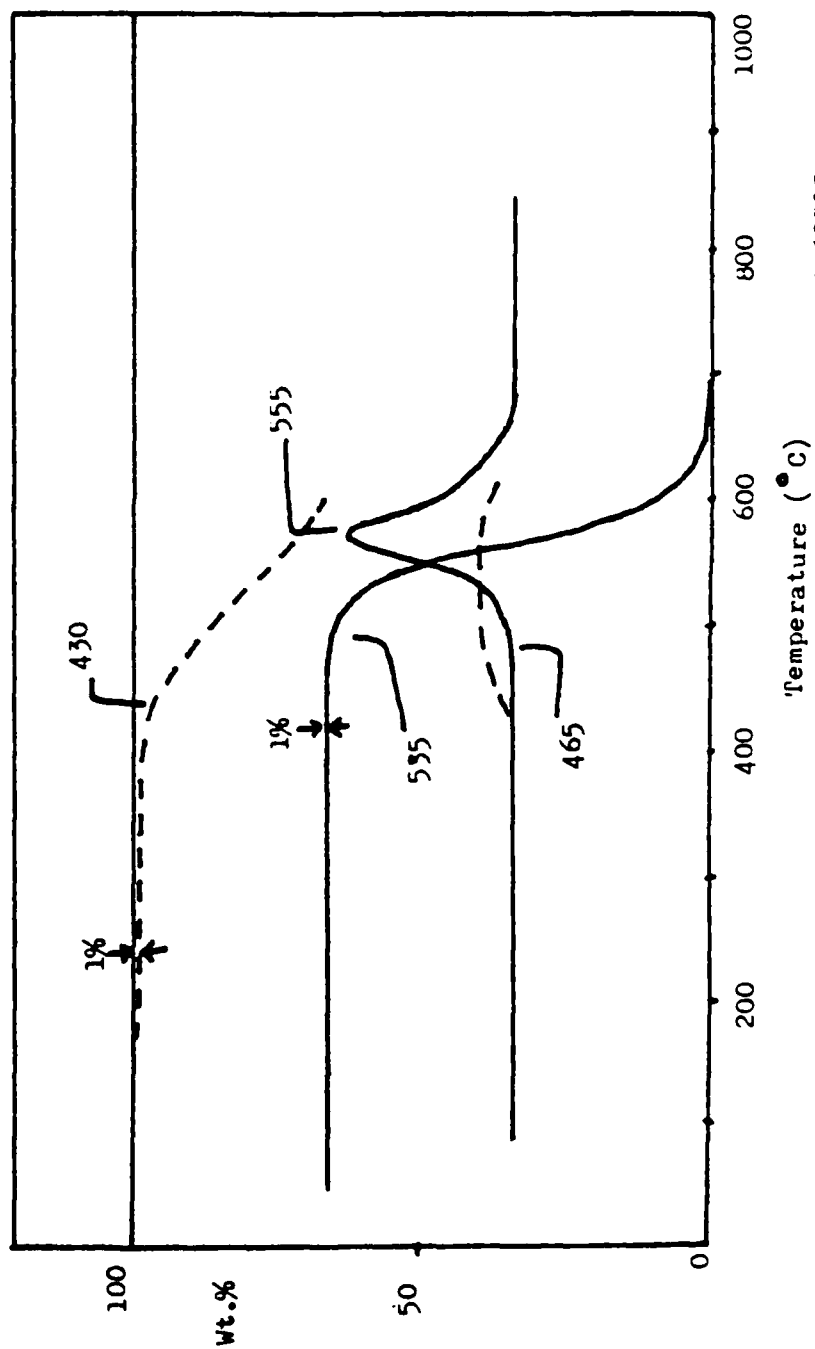


FIGURE 17 TGA IN AIR OF ATS_G, PREDEGRADED UNDER HELIUM TO 600°C

Heating Rate 5°C/min

Sample Size 15.85 mg

--- Helium

— Air

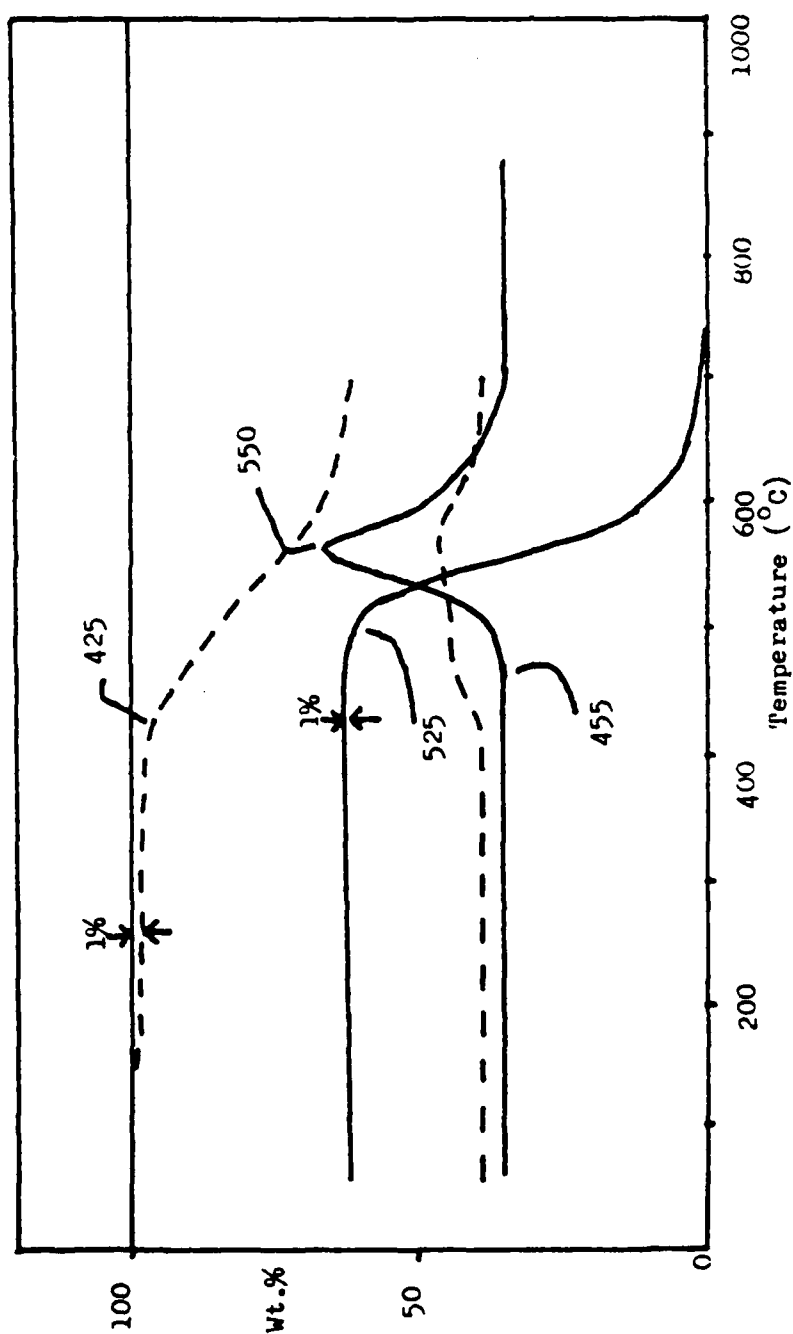


FIGURE 18 TGA IN AIR OF ATS-G, PREDEGRADED UNDER HELIUM TO 700°C

Heating Rate 5°C/min

Sample Size 19.50 mg

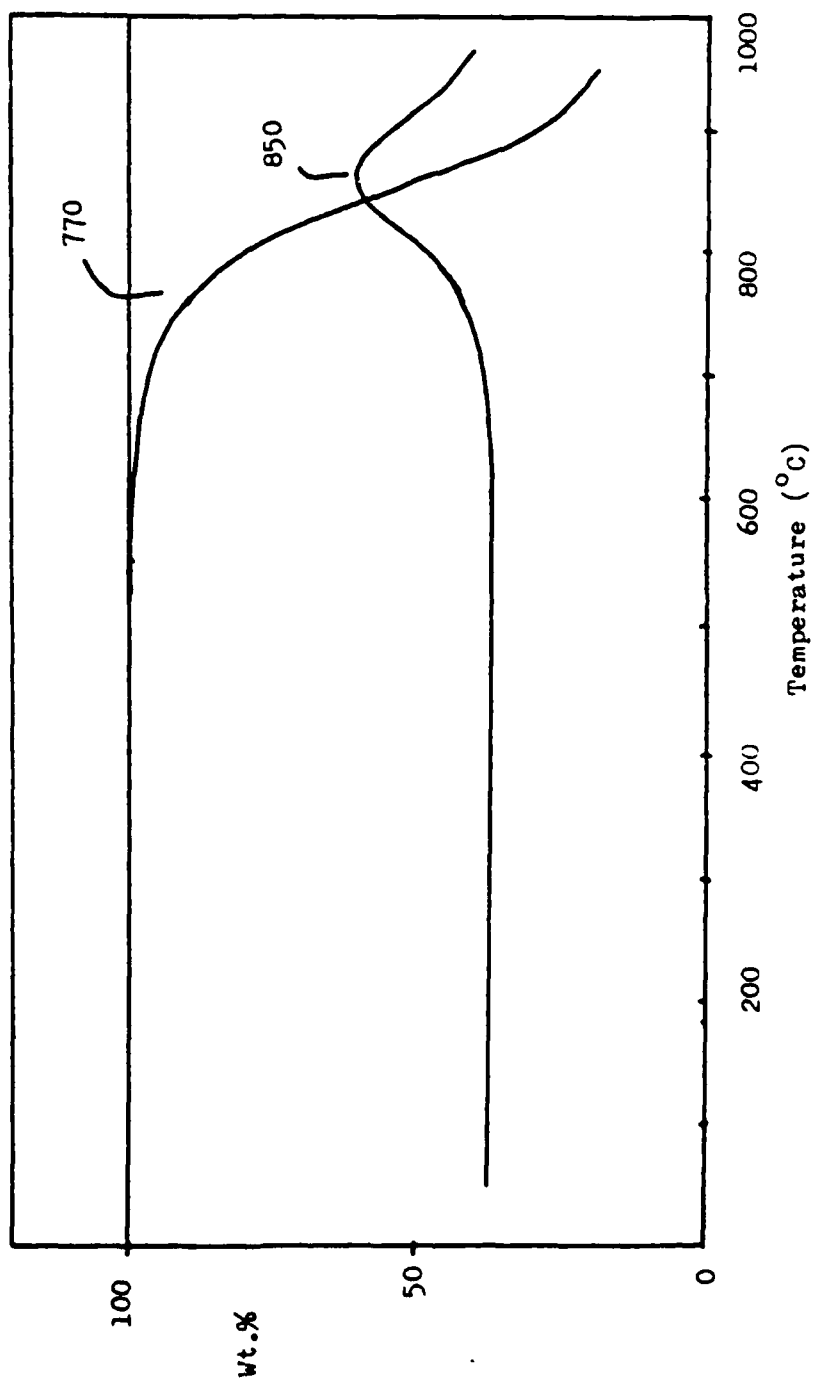


FIGURE 19 TGA OF GRAPHITE IN AIR

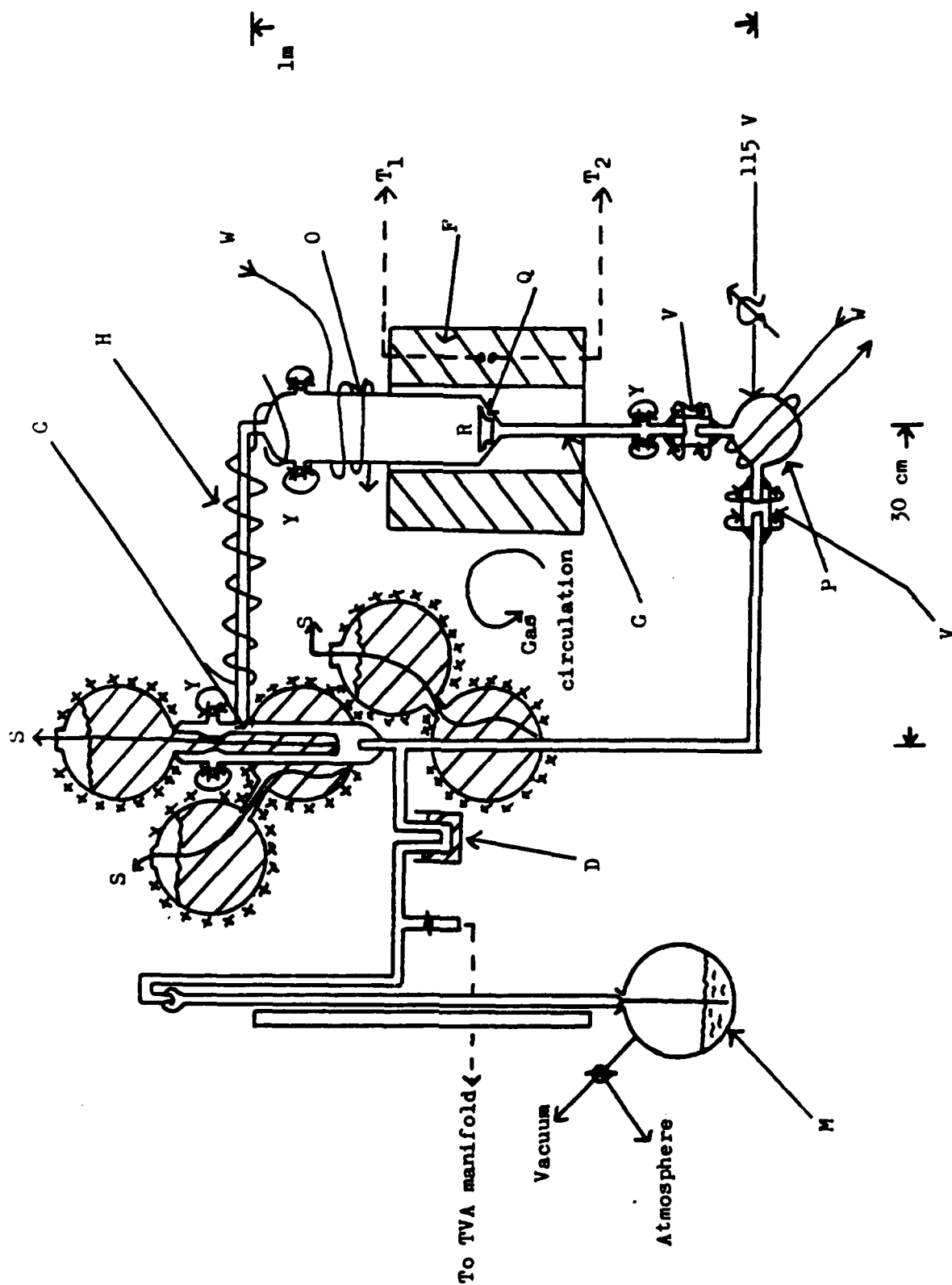


FIGURE 20a OXIDATION REACTOR



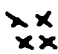
P	Sealed in Magnetic Drive Pump
	Clamp
Y	Flange Joint With Viton "O" Ring Seal
	Liquid Nitrogen
S	Liquid Nitrogen Siphon Tubes (To House Vacuum)
	Polyurethane Insulating Foam Over Polyethylene Film
H	Electrical Heating Tape
F	Tubular Muffle Furnace (RT - 1000°C)
W	Water Filled Copper Cooling Coils
Q	Quartz Degradation Tube and Crucible with Fluted Base
R	Residue Of Degradation
O	The Oligomeric Product Fraction Of Degradation
C	The Condensable Gas Product Fraction Of Degradation
G	Gas Preheat Tube
V	Rubber Vacuum Tubing Sealed With Dow Corning "Silastic 732"
	Curable Silicone Rubber
D	Dewar Flask
M	Mercury Manometer With Meter Stick
T ₁	Cr/Al Thermocouple To Oven Programmer
T ₂	Cr/Al Thermocouple To Recorder

FIGURE 20b KEY TO FIGURE 20a

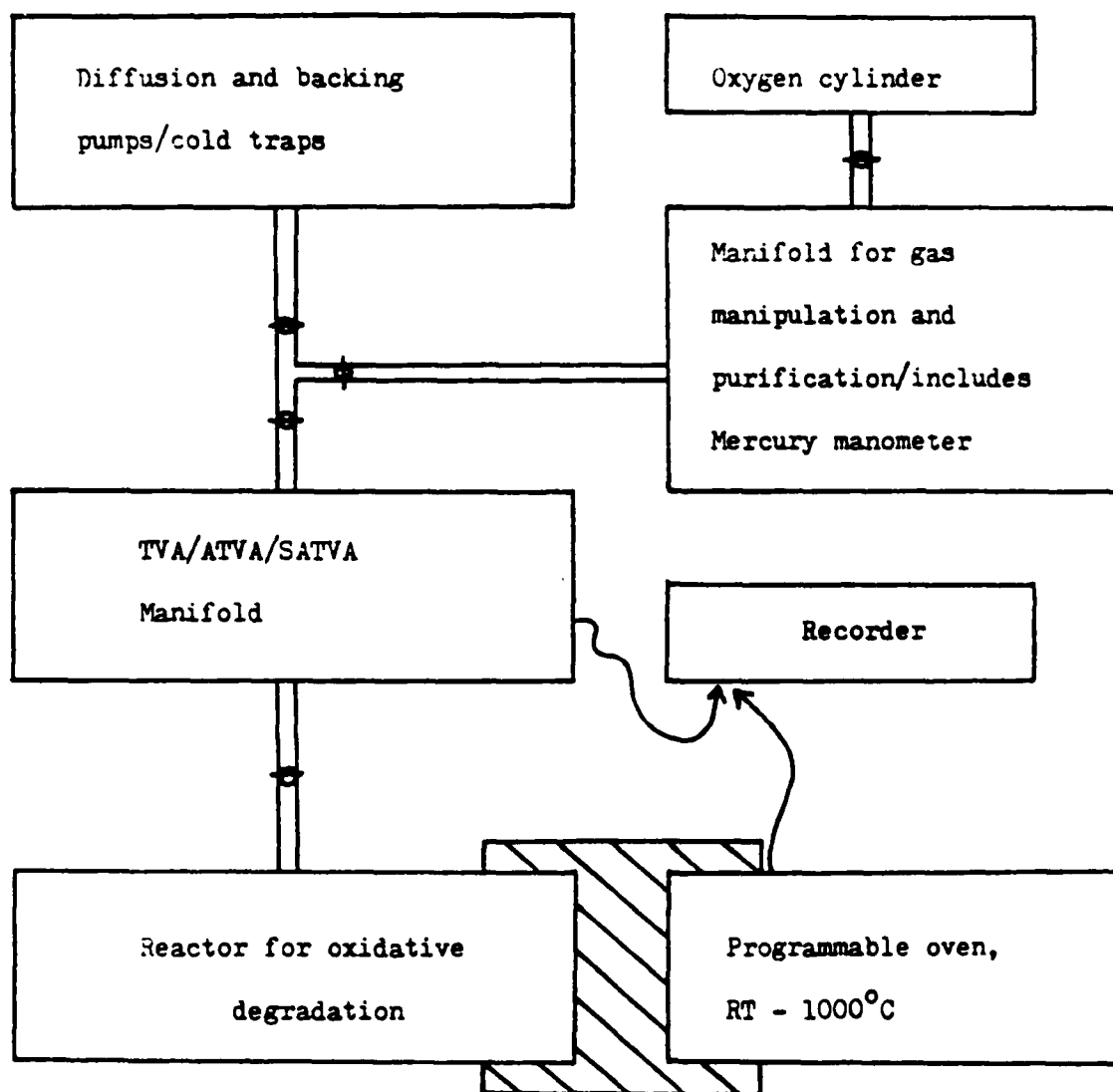


FIGURE 21 VACUUM MANIFOLD SCHEMATIC

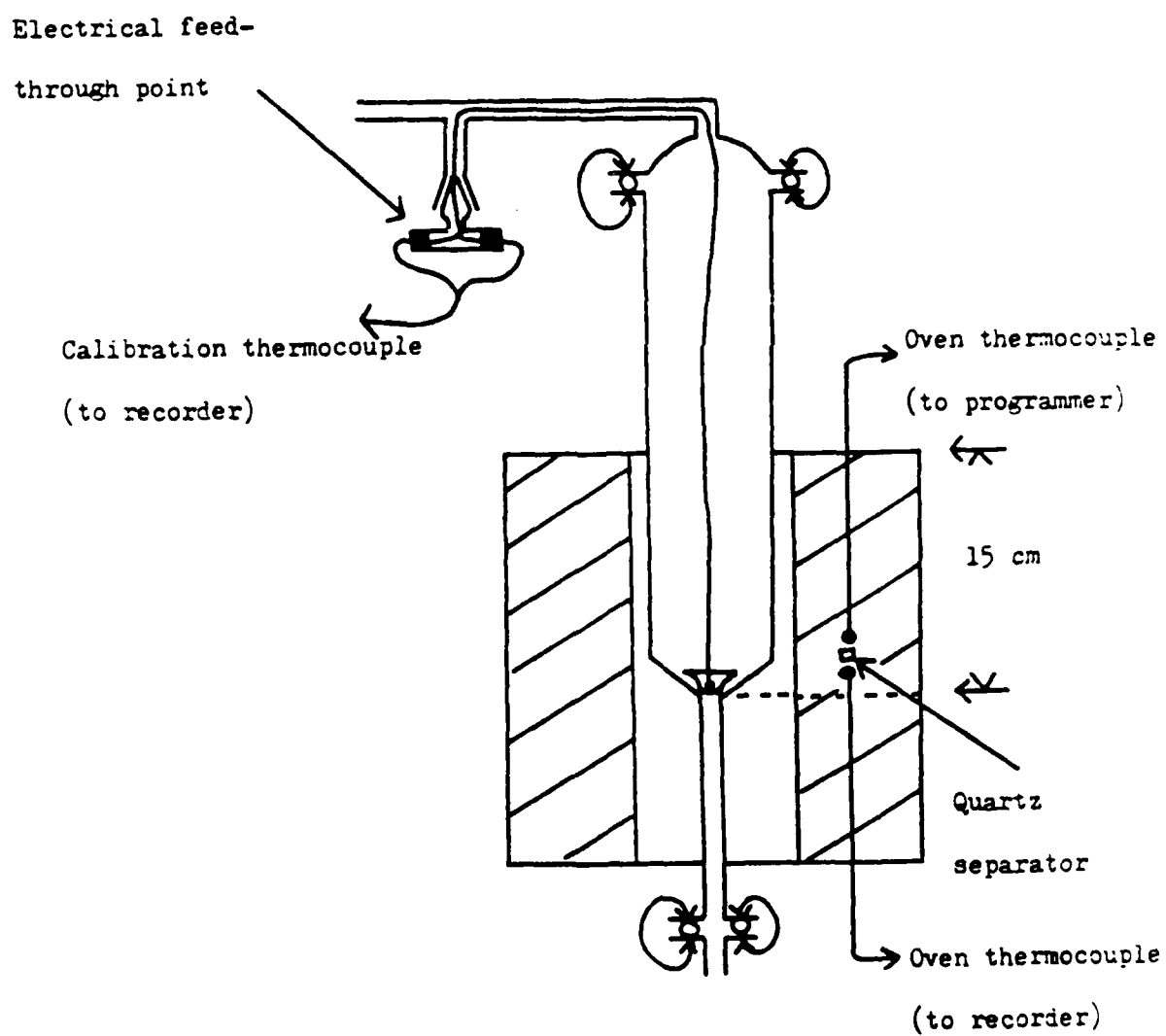


FIGURE 22 ASSEMBLY FOR OVEN CALIBRATION

Initial Oxygen Pressure - 1 cm Hg

Heating Rate - $5^{\circ}\text{C}/\text{min}$

Crucible - 15 cm into Oven

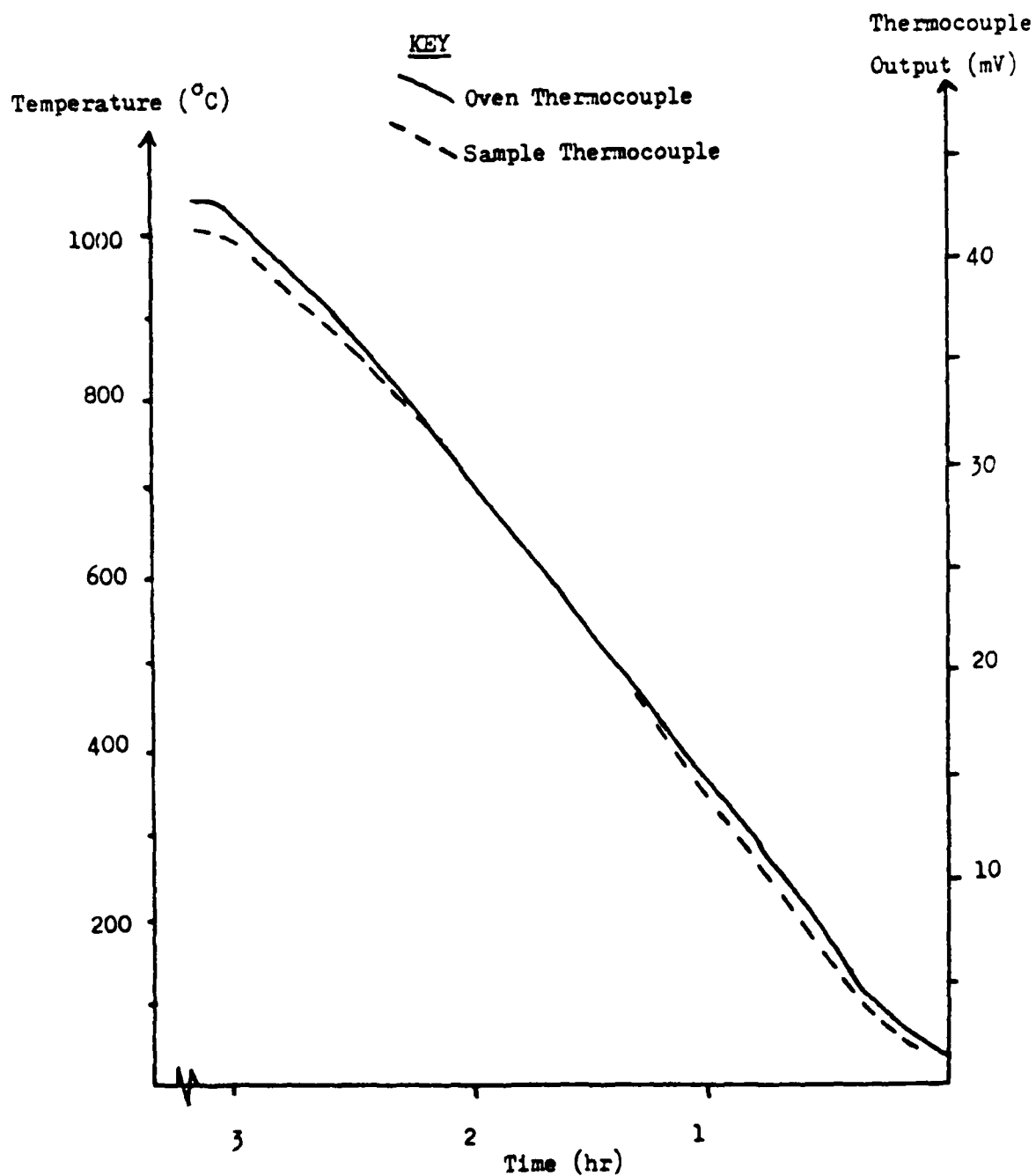


FIGURE 23 OVEN CALIBRATION CURVE FOR OXIDATION REACTOR

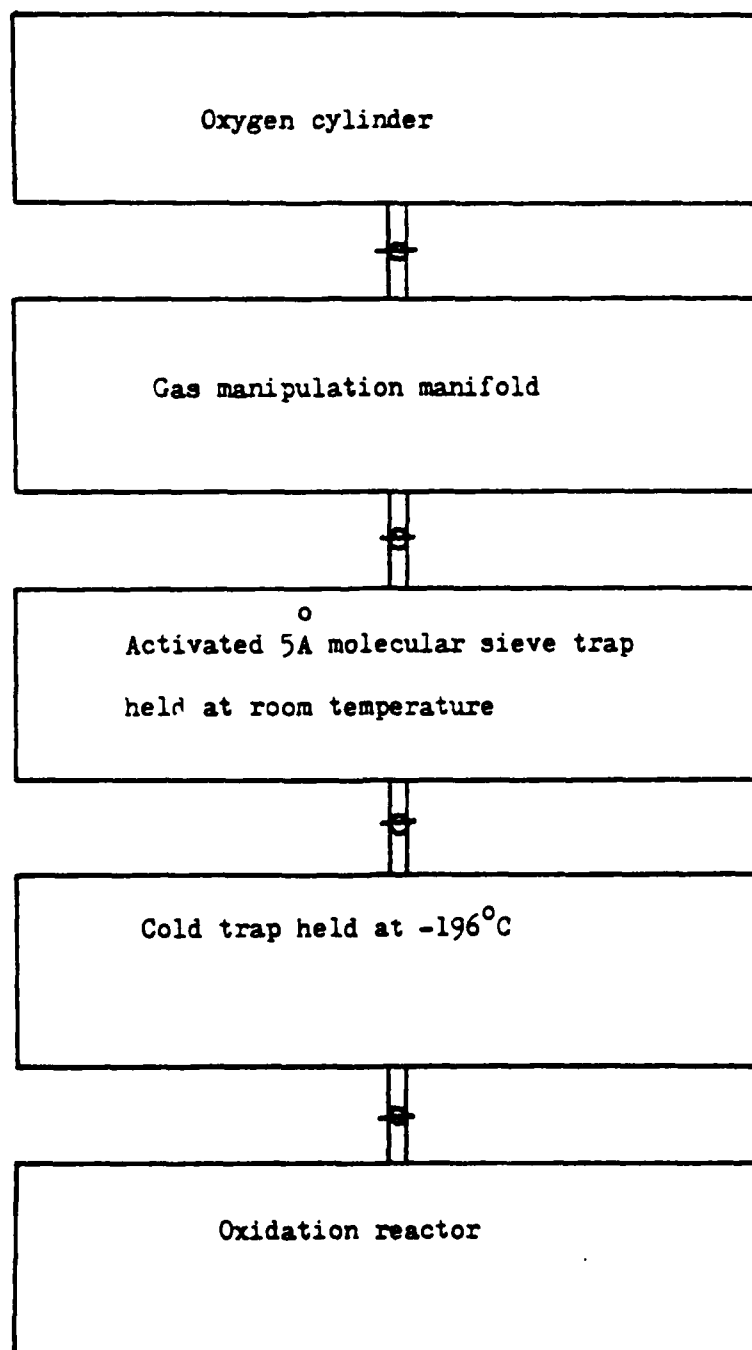


FIGURE 24 GAS PURIFICATION TRAIN SCHEMATIC

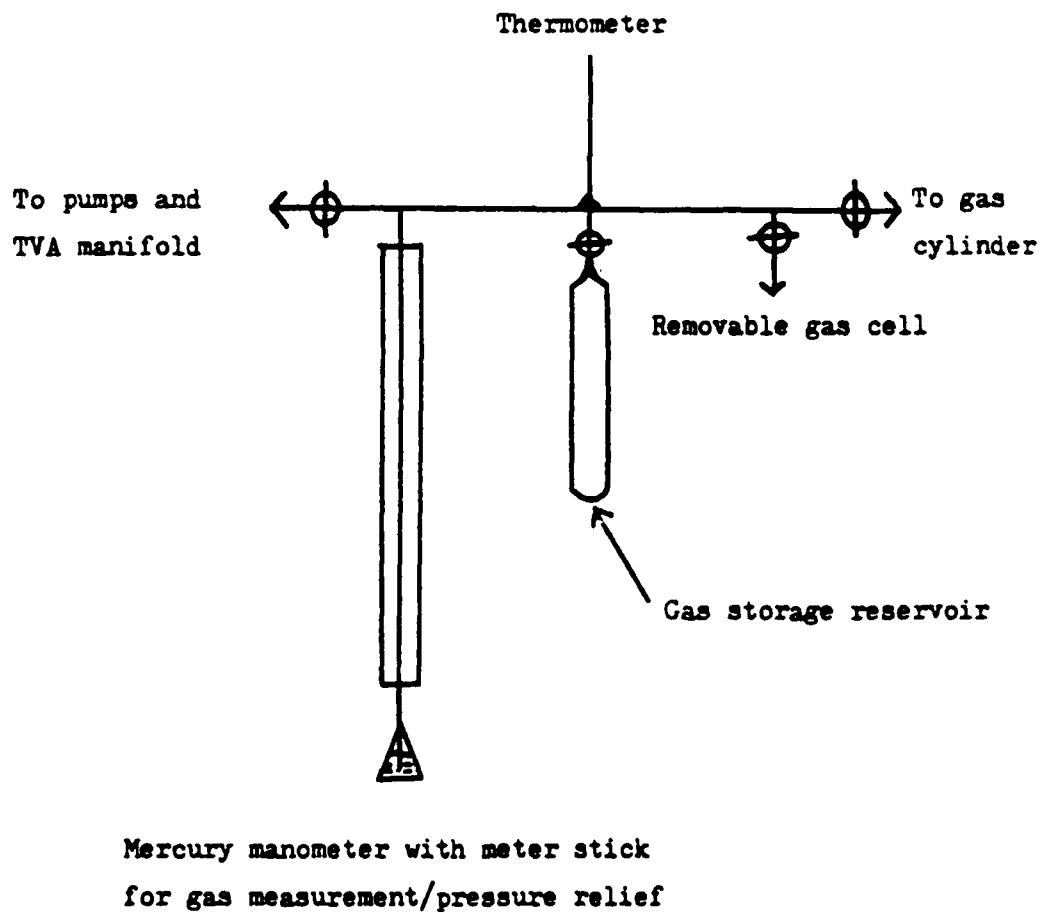


FIGURE 25 GAS MANIPULATION MANIFOLD

KEY

- - - (-) Thermocouple Output (Trap Temperature)

— Pirani Output (Pressure)

1 CO_2

2 Benzene

3 Water

4 Phenol

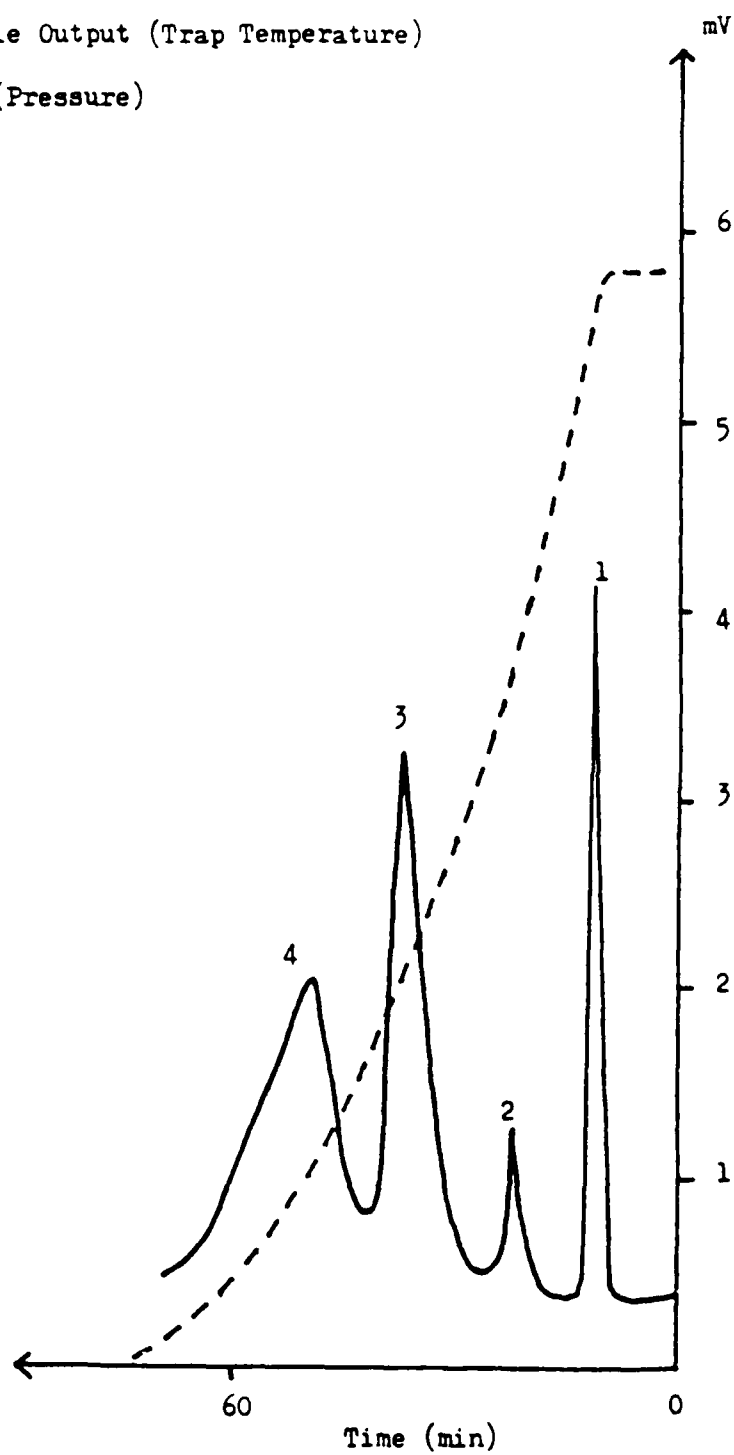


FIGURE 26 SATVA OF CONDENSABLE VOLATILES COLLECTED IN BLANK RUN TO 800°C

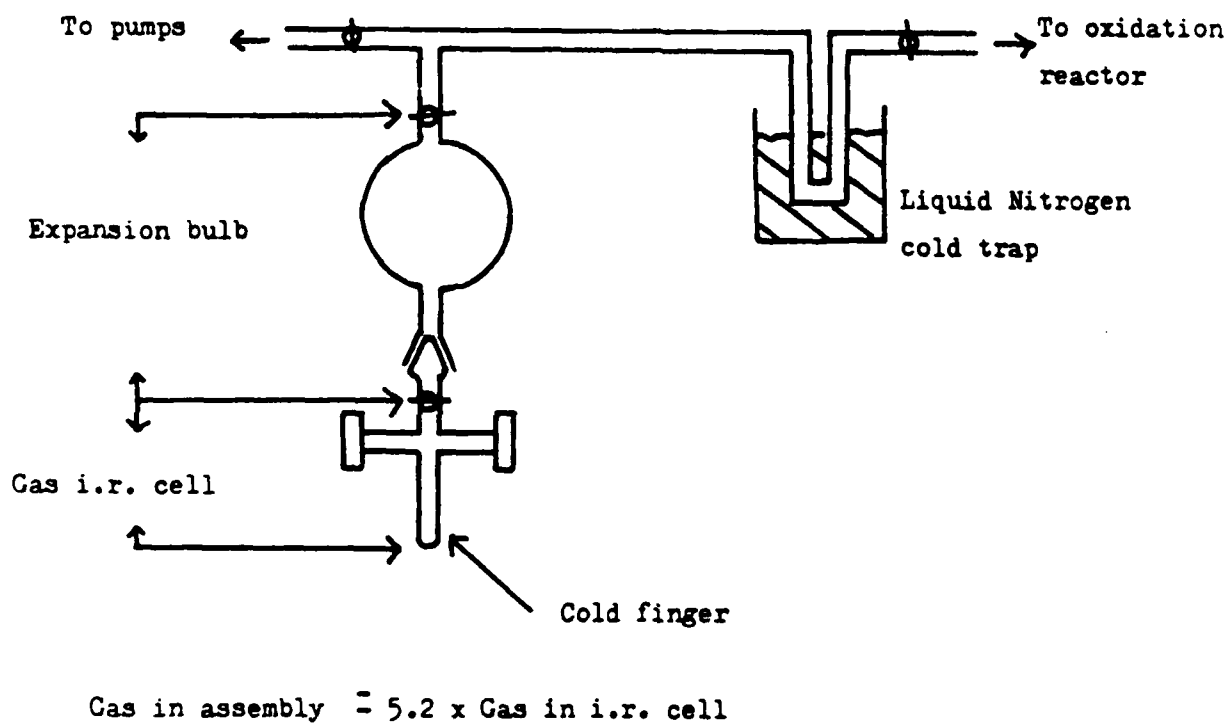


FIGURE 27 CALIBRATED CONTAINER FOR QUANTITATIVE GAS PHASE
I.R. ANALYSIS OF CONDENSABLE VOLATILE PRODUCTS OF
OXIDATION

KEY

I Calibration Spectra

II Condensable Volatile Products Of
Oxidation To 800°C Of ATS-G

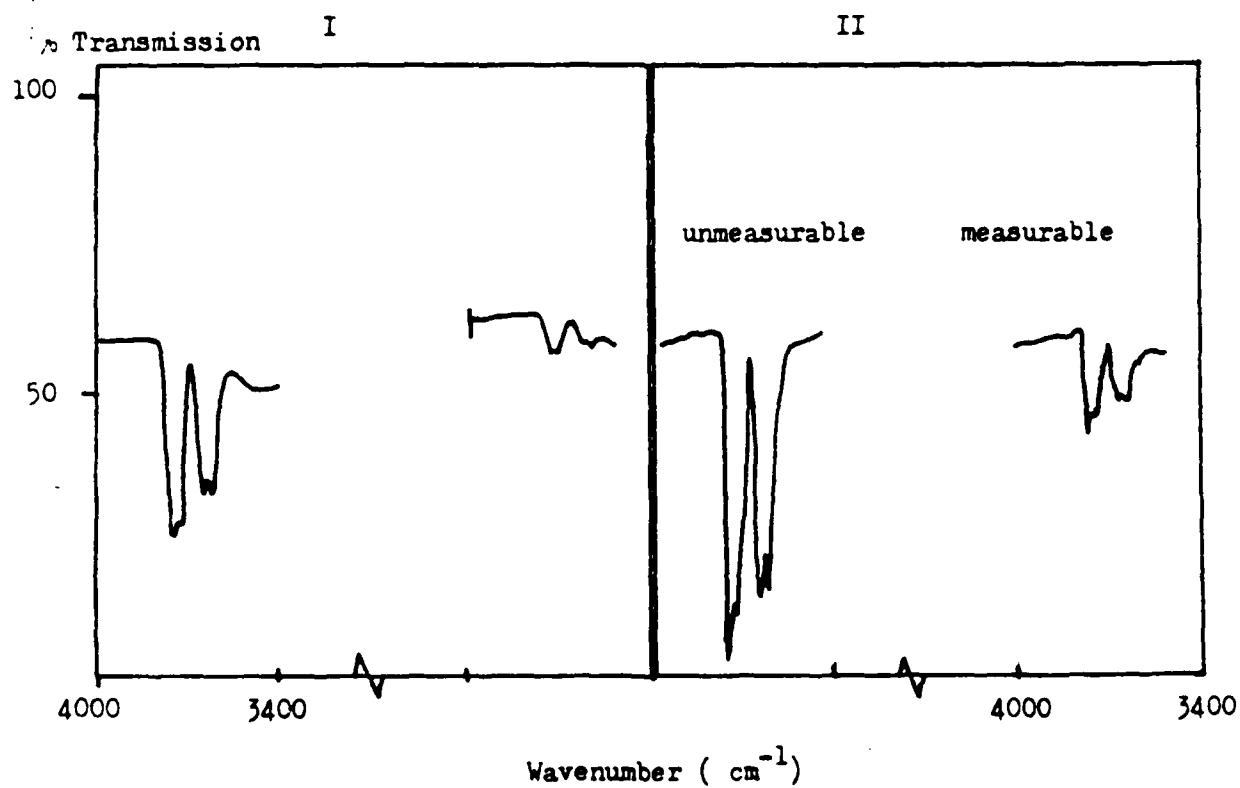


FIGURE 28 GAS PHASE I.R. SPECTRA OF CARBON DIOXIDE, BEFORE AND AFTER EXPANSION INTO CALIBRATED CONTAINER

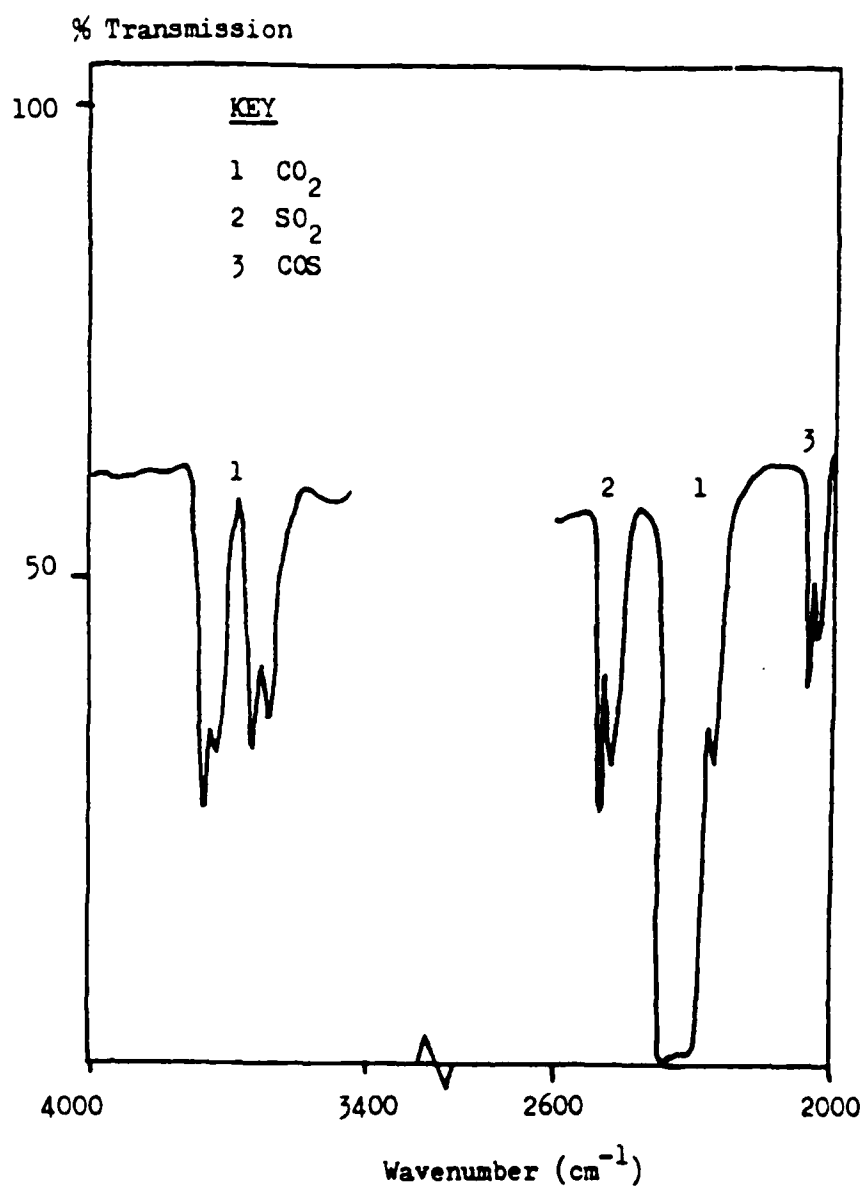


FIGURE 29 GAS PHASE I.R. SPETRUM OF THE CONDENSABLE VOLATILE PRODUCTS OF OXIDATION TO 800°C OF PRECURED ATS-G

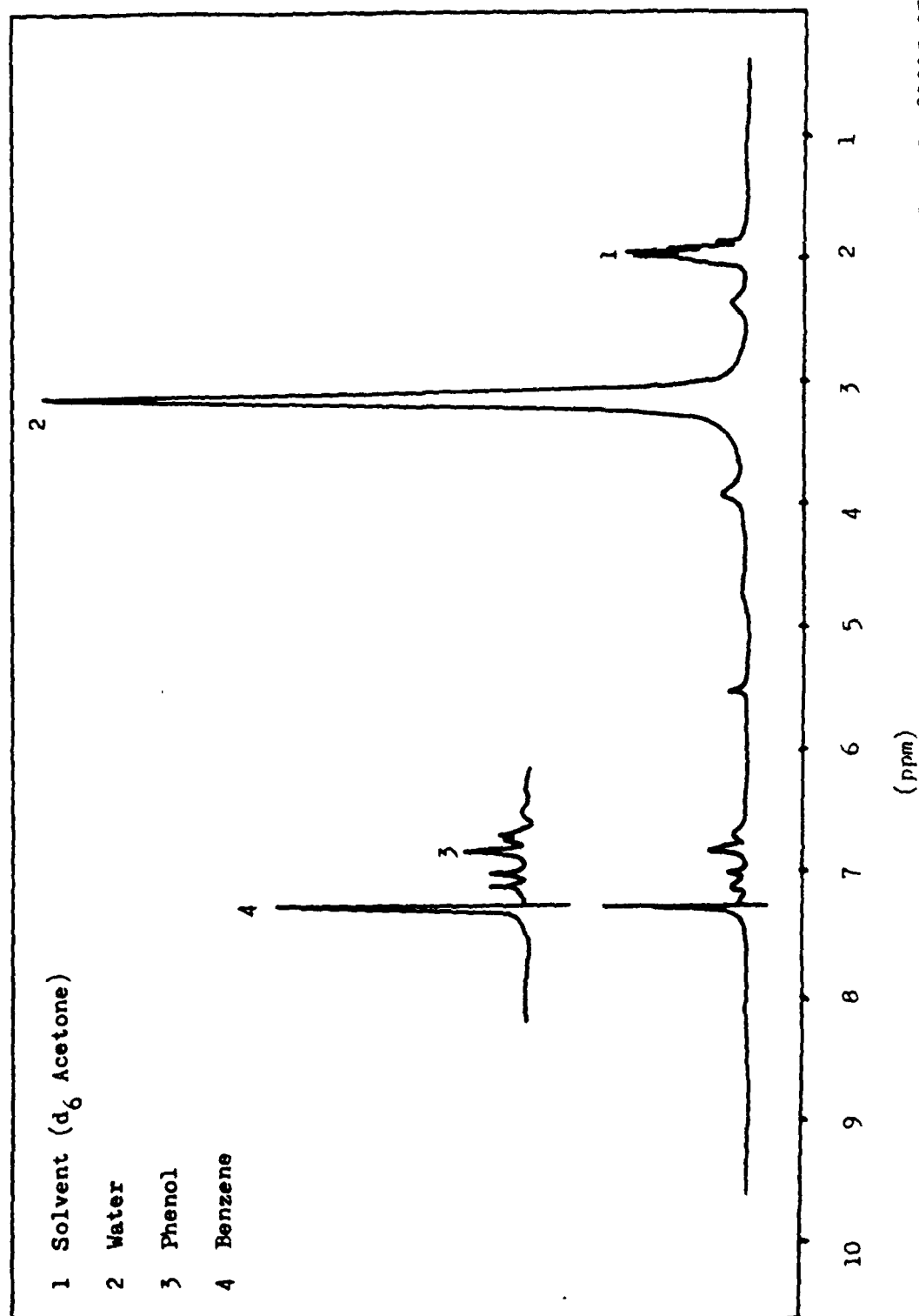


FIGURE 30 PROTON N.M.R. SPECTRUM OF THE CONDENSABLE VOLATILE PRODUCTS OF OXIDATION TO 800°C OF PRECURED ATS-G

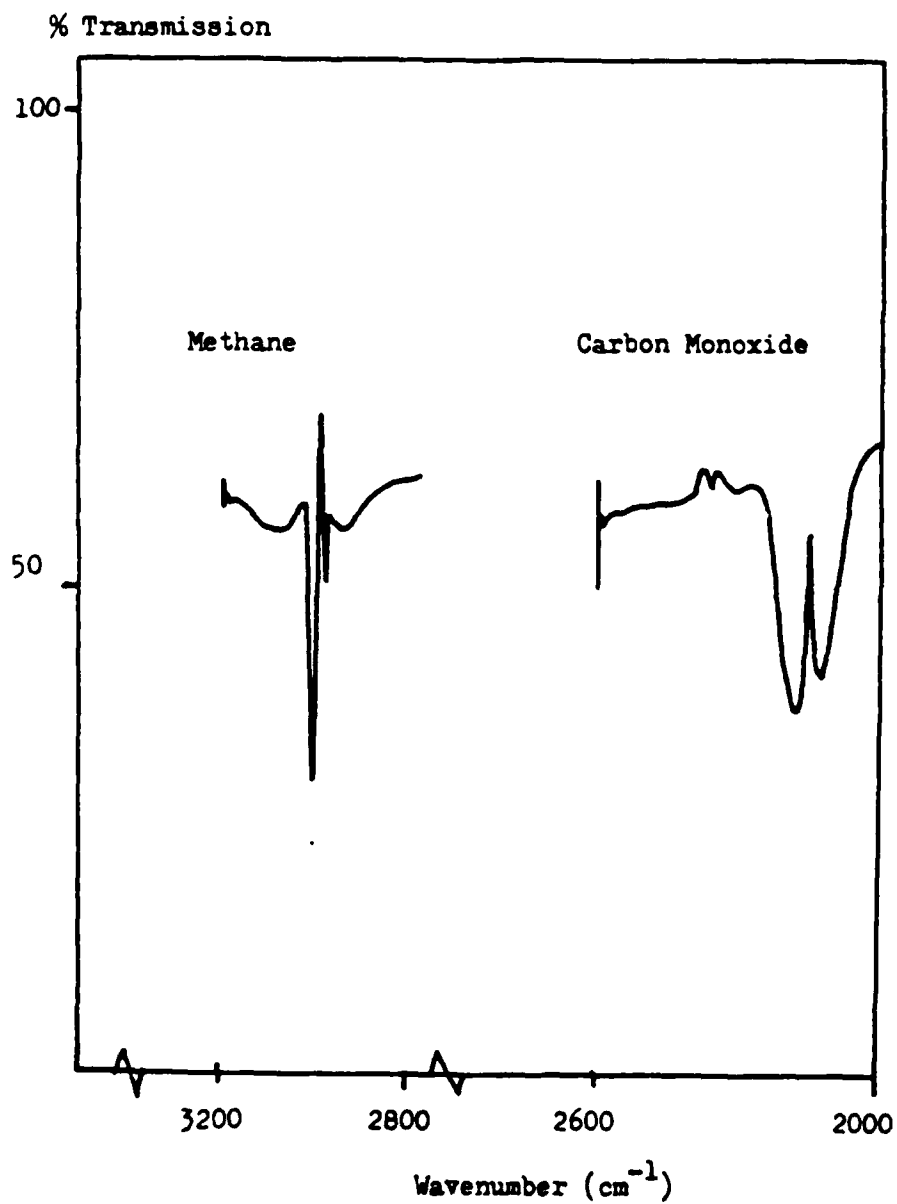


FIGURE 31 GAS PHASE I.R. SPECTRUM OF THE NONCONDENSABLE VOLATILE PRODUCTS OF OXIDATION TO 800°C OF PRECURED ATS-G

KEY

--- (-) Thermocouple Output (Trap Temperature)

— Pirani Output (Pressure)

1 CO_2 , COS

2 SO_2

3 Benzene

4 Water

5 Phenol

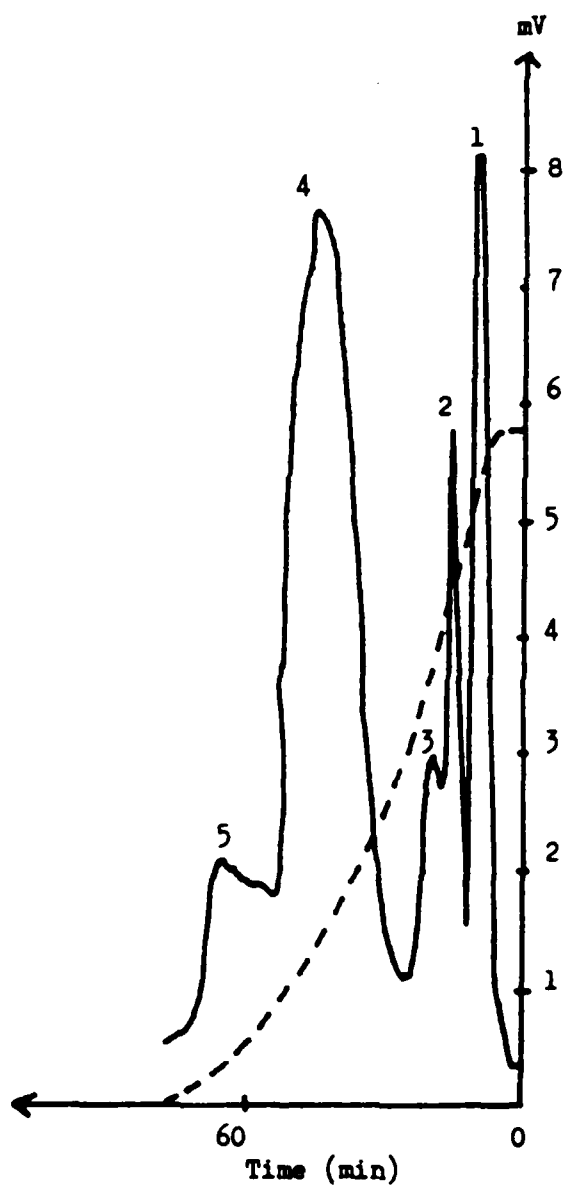


FIGURE 32 SATVA OF CONDENSABLE VOLATILE PRODUCTS OF OXIDATION TO 800°C OF 50mg PRECURED ATS-G

KEY

---(-) Thermocouple Output (Trap Temperature)

— Pirani Output (Pressure)

1 CO₂

2 COS

3 SO₂

4 Benzene

5 Water

6 Phenol

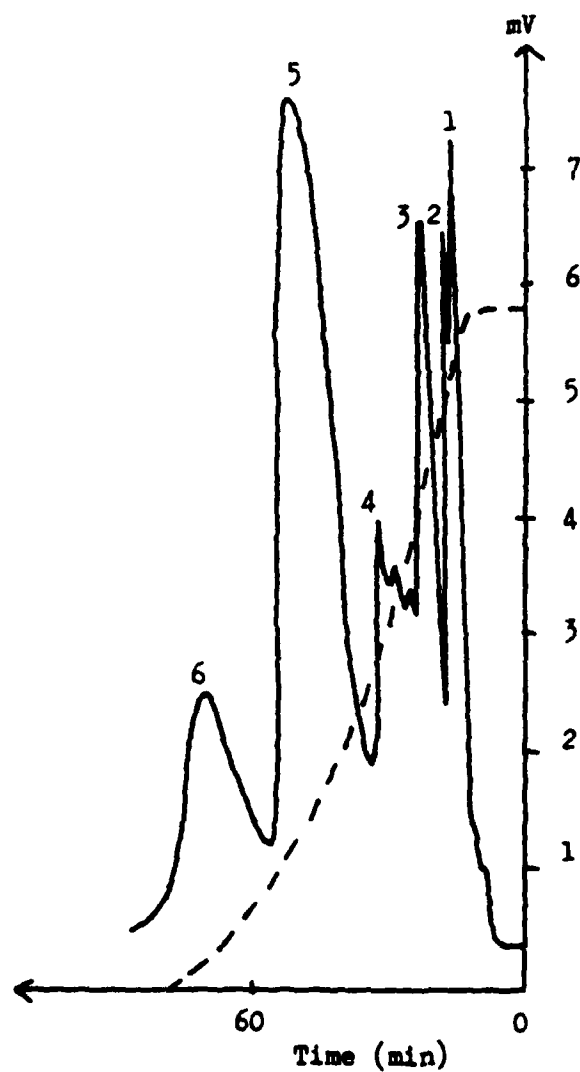


FIGURE 33 SATVA OF CONDENSABLE VOLATILE PRODUCTS OF OXIDATION
TO 800°C OF 100mg PRECURED ATS-G

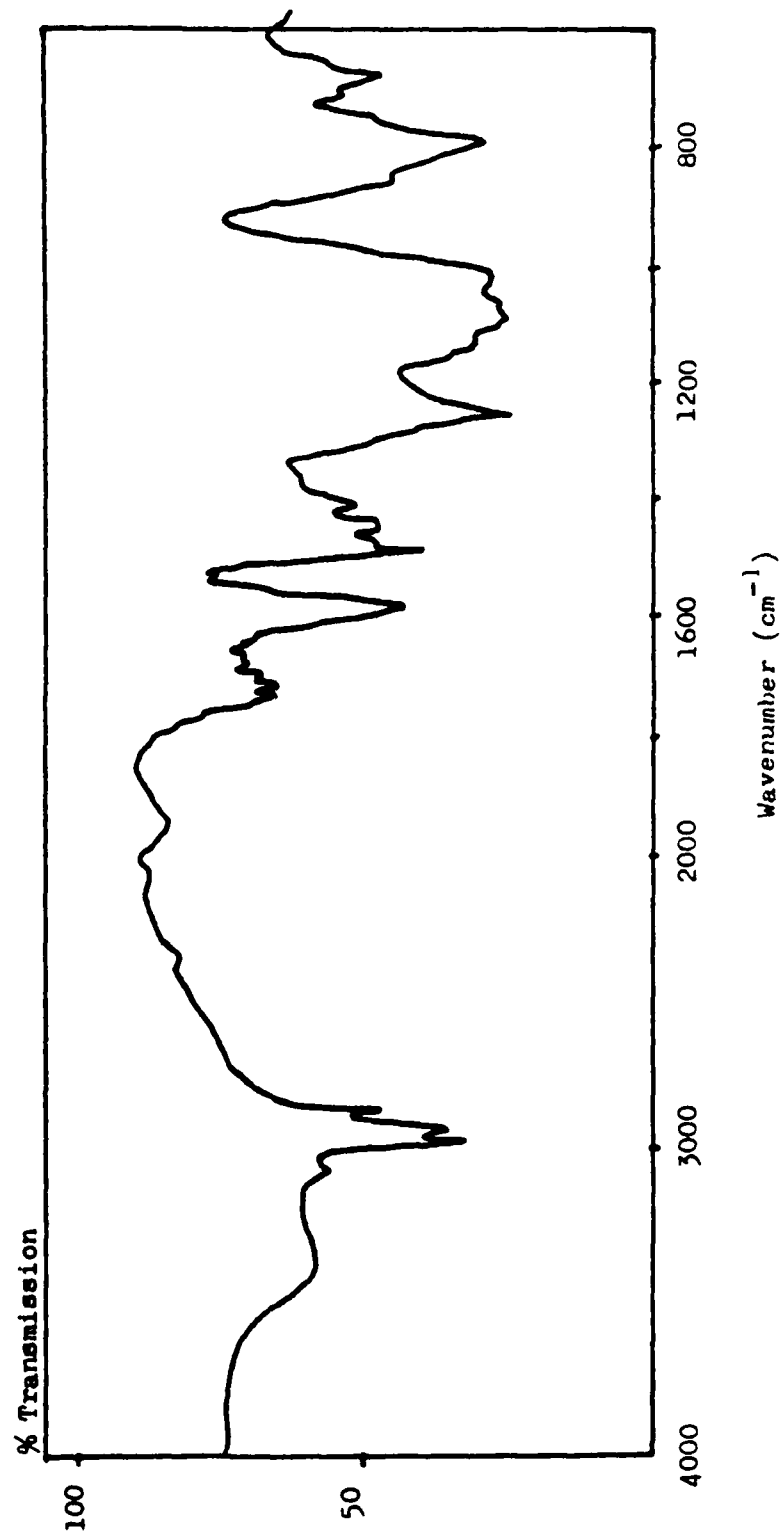


FIGURE 34 I.R. SPECTRUM OF THE OLIGOMERIC PRODUCT FRACTION OF OXIDATION TO 800°C OF PRECURED ATS-G

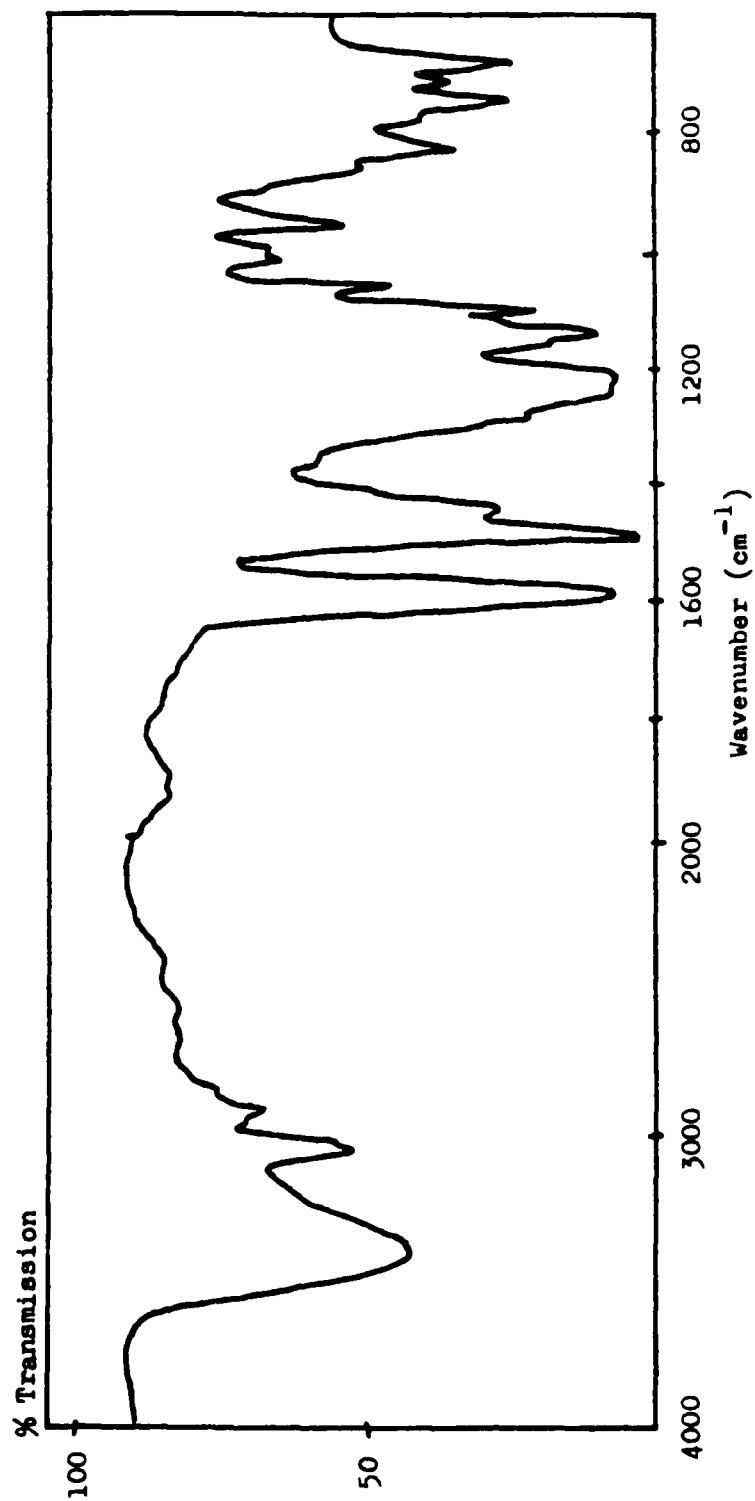


FIGURE 35 I.R. SPECTRUM OF THE OLIGOMERIC PRODUCT FRACTION OF THERMAL DEGRADATION TO 1020°C OF PRECURED ATS-G

KEY

- - - (-) Thermocouple Output (Trap Temperature)

— Pirani Output (Pressure)

1 CO₂

2 Benzene

3 Water

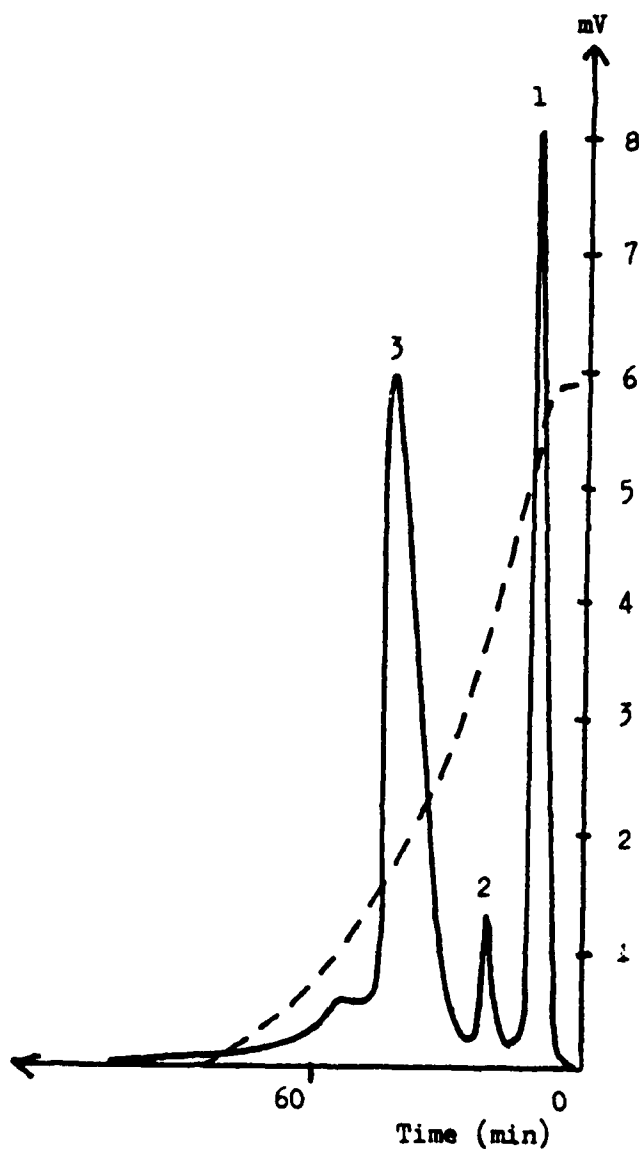


FIGURE 36 SATVA OF CONDENSABLE VOLATILE PRODUCTS OF
OXIDATION TO 700°C OF ATS-G, PREDEGRADED
UNDER VACUUM TO 700°C